

1 **Novel prokaryotic sensing and regulatory system employing previously unknown**
2 **nucleic acids-based receptors**

3

4 Victor Tetz¹ and George Tetz^{1*}

5

6

7 ¹Human Microbiology Institute, New York, NY 10013, USA.

8

9

10 *Correspondence and requests for materials should be addressed to GT (email:
11 g.tetz@hmi-us.com)

12

13

14

15

16

17

18

19

20

21

22

23

24

25

26

27

28

29

30

31

32

33

34

35

36

37

38 **Abstract**

39 The present study describes a previously unknown universal signaling and regulatory system,
40 which we named TRB receptor system. This system is responsible for sensing, remembering,
41 and regulating cell responses to various chemical, physical or biological stimuli. It controls cell
42 survival, variability, reproduction, adaptation, genome changes, and gene transfer. Importantly,
43 the TRB-receptor system is responsible for the formation and maintenance of cell memory, as
44 well the ability to “forget” preceding events. The system is composed of DNA- and RNA-based
45 receptors located outside the membrane named “TezRs”, as well as reverse transcriptases and
46 integrases. The sensory and regulatory functions of TezRs enable the TRB-receptor system to
47 control all major aspects of bacterial behavior, such as growth, biofilm formation and dispersal,
48 utilization of nutrients including xenobiotics, virulence, chemo- and magnetoreception, response
49 to external factors (e.g., temperature, UV, light and gas content), mutation events, phage-host
50 interaction and recombination activity. Additionally, it supervises the function of other receptor-
51 mediated signaling pathways. Transcriptome analysis revealed that the loss of different TezRs
52 instigates significant alterations in gene expression.

53

54 **HIGHLIGHTS**

55 The TRB-receptor system regulates bacterial sensing and response to various stimuli.

56 The TRB-receptor system is responsible for maintenance and loss of cell memory.

57 The TRB-receptor system comprises DNA- and RNA-based “TezRs” receptors.

58 The TRB-receptor system relies on reverse transcriptases and recombinases.

59 The TRB-receptor system oversees other receptor-mediated signaling pathways.

60 TezRs are implicated in cell mutation and recombination events.

61

62

63

64

65

66

67

68

69

70 INTRODUCTION

71 To ensure survival, bacteria need to adapt to a constantly changing environment. Yet, the details
72 of sensory and biophysical processes involved in reception have remained elusive (1–3). At
73 present, these adaptations are known to be mediated by a variety of predominantly
74 transmembrane receptors consist of a protein structure, which control different key aspects of the
75 interaction with the environment, cell-to-cell signaling, and multicellular behavior.
76 Chemoreceptors represent the most well studied type of bacterial receptors (3–7). They recognize
77 various signals, primarily growth substrates or toxins (8,9). Chemoreception is tightly linked to
78 chemotaxis and provides bacteria with the capacity to approach or escape different compounds,
79 thus favoring the movement toward optimal ecological niches (10). However, many aspects of
80 chemoreception remain unclear, including details of the mechanisms underlying high sensitivity,
81 sensing of multiple stimuli, and recognition of previously unknown nutrients or xenobiotics (11–
82 13).

83 Bacterial receptive function and interaction with the environment is coupled to bacterial memory,
84 another poorly characterized phenomenon (14–20).

85 Cell memory is viewed as a part of history-dependent behavior and is intended as a means for
86 the efficient adaptation to recurring stimuli. It can be encoded by membrane potential, which is
87 also associated with transmembrane receptors in bacteria (21).

88 Sensing of physical factors by bacteria remains even more elusive. For example, the mechanism
89 of magnetoreception, whereby microorganisms sense the geomagnetic field, has been well
90 described only in magnetotactic bacteria (22). These prokaryotes sense magnetic fields due to
91 the biomineralization of nano-sized magnets, termed magnetosomes, within cells (23, 24).
92 However, existing studies have not explained why bacteria lacking these elements could still
93 sense the magnetic field (25, 26). Recent data suggest that intracellular DNA can be affected by
94 magnetic fields and is able to interact with them, but the nature of such interactions remains
95 enigmatic (27–29).

96 The mechanism and regulation of bacterial temperature sensing is also characterized by
97 numerous unknowns. Different studies have pointed to Tar/Tsr receptors as responsible for
98 controlling and regulating the temperature response, but the detailed mechanisms of their
99 reception remain elusive (30–33). Some authors also highlight the sensing of the temperature
100 that is associated with blue-light sensing through the BlsA Sensor (34,35).

101 Therefore, the question of how known receptors sense a diverse array of chemical, biological,
102 and physical factors remains insufficiently explored. It has been suggested that certain protein
103 receptors could be organized into sensory arrays, whereby cooperative interactions between
104 receptors enable the sensing of a diverse range of stimuli (7,36–39). Still, even such clusters

105 could not account for the totality of different stimuli sensed by bacteria. Even in the case of known
106 receptive systems it remains to be determined how bacteria sense the whole plethora of available
107 environmental factors including previously unknown exogenous stimuli, how remote sensing
108 operates, what is the common sensor part of most receptors, and how signal transduction is
109 mediated. Therefore, a better understanding of receptors and receptor systems could expand our
110 knowledge of the regulation of bacterial physiology, virulence, and adaptation.

111 In this work, we report for the first time the identification of novel bacterial elements constituted
112 by nucleic acid molecules (located outside the cell membrane and presumably also inside the
113 cell), which can sense and amplify the signals from different chemical, physical, and biological
114 stimuli into an integrated output (40). Because they possess the features of receptors and
115 regulators, we named these elements Tezeled Receptors (TezRs). Here, we confirmed their
116 receptor and regulatory activities, and also revealed their participation in cell memory formation,
117 maintenance, and loss. Finally, we demonstrated that TezRs were part of a previously unknown
118 receptor system, which we named TezR-based receptor system (TRB-receptor system).

119

120 **RESULTS**

121 **Nucleases remove cell surface-bound nucleic acids**

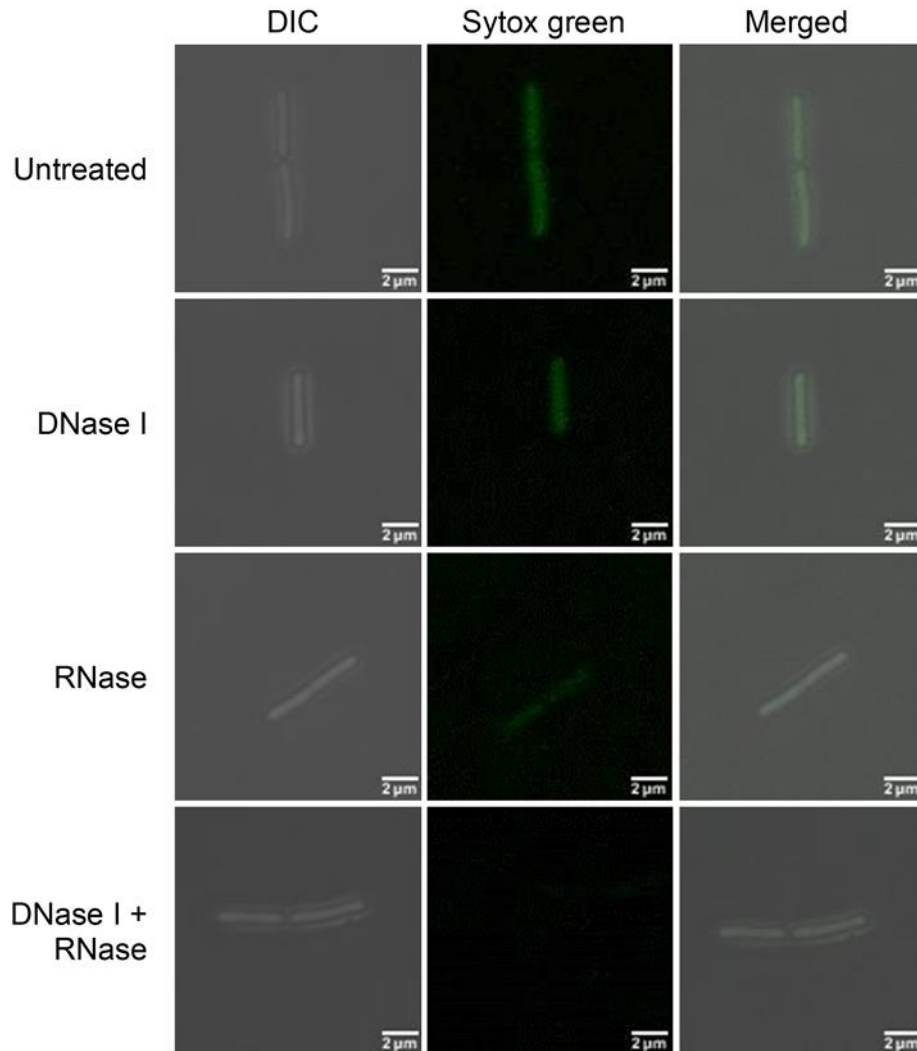
122 First, we confirmed the destruction of cell-surface bound DNA and RNA by studying the changes
123 in fluorescence of washed planktonic *B. pumilus* VT1200 following their treatment with 10 µg/mL
124 DNase I and RNase A for 15 min or a combination of the two. SYTOX Green-stained *B. pumilus*
125 displayed clear green fluorescence, confirming the presence of cell surface-bound nucleic acids,
126 which were not removed upon washing of culture medium or matrix (Fig. 1A, B).

127 Bacteria treated with either DNase or RNase alone exhibited a decrease, but not the total
128 disappearance of fluorescence compared to untreated cells ($p < 0.0001$). Instead, bacteria treated
129 with a combination of DNase and RNase revealed the total disappearance of surface fluorescence
130 compared to single-nuclease treatment ($p < 0.0001$).

131 As it was outside the scope of our study to evaluate which part of the cell surface-bound DNA or
132 RNA exerted receptive functions, in the following experiments we applied the same nuclease
133 treatment regimen that resulted in total removal of all cell surface-bound nucleic acids as
134 observed here.

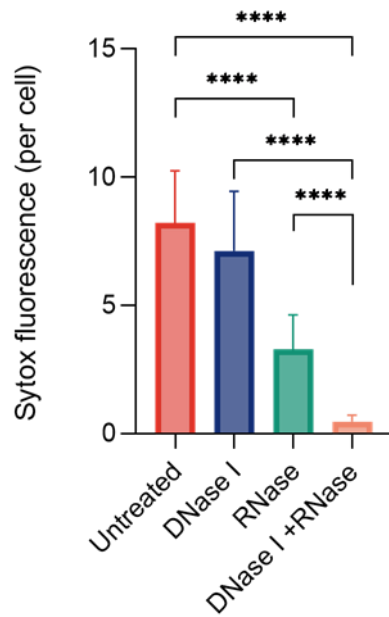
135 Next, we verified that the RNase A used in this study was not internalized by the bacteria. To
136 examine the ability of RNase A to penetrate the bacterial cell wall we linked the enzyme with a
137 fluorophore. To score the penetration capability of RNase in *B. pumilus* we incubated *B. pumilus*
138 on agar media supplemented with fluorophore-linked RNase or cultivated pre-treated *B. pumilus*

139 with the same RNase. However, in both experiments no signs of RNase internalization were
140 observed. (Supplementary Fig. 1).



141

142 A



143

144 B

145 **Figure 1.** Removal of *B. pumilus* cell surface-bound DNA and RNA molecules with nucleases.

146 Green fluorescence denotes cell surface-bound DNA and RNA of *B. pumilus* stained with the
147 membrane impermeable SYTOX Green dye. (A) DIC (left), SYTOX Green (center), and merged
148 (right) images of untreated and DNase/RNase-treated *B. pumilus* at 100x magnification. Scale
149 bars represent 2 μ m. (B) Quantification of SYTOX Green signal intensity per cell (n = 10; mean \pm
150 SD). **** p < 0.0001, two-tailed unpaired *t*-tests.

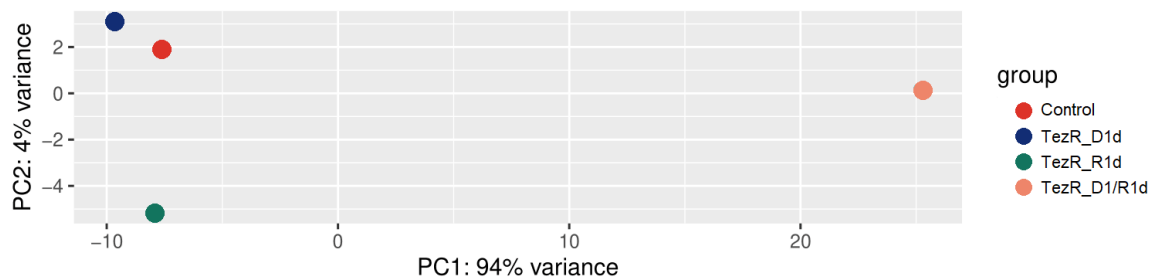
151

152 **TezR destruction has a global impact on gene expression**

153 To gain insight into the consequences of TezRs loss on bacterial gene expression, RNA-seq
154 analyses of *S. aureus* gene expression profile were examined following the removal of primary
155 TezRs. Principal-component analysis (PCA) showed that *S. aureus* due to the loss of primary
156 TezRs clustered separately from the control group of *S. aureus* where TezRs was intact. The
157 largest difference in PCA was observed for *S. aureus* TezR_R1^d (Fig. 2A). These differences in
158 gene expression datasets are also clearly evident in the hierarchical clustering and heatmaps of
159 Euclidean distance. Strikingly, the largest pairwise Euclidean distance was observed between
160 the control *S. aureus* and TezR_R1^d (Fig. 2B).

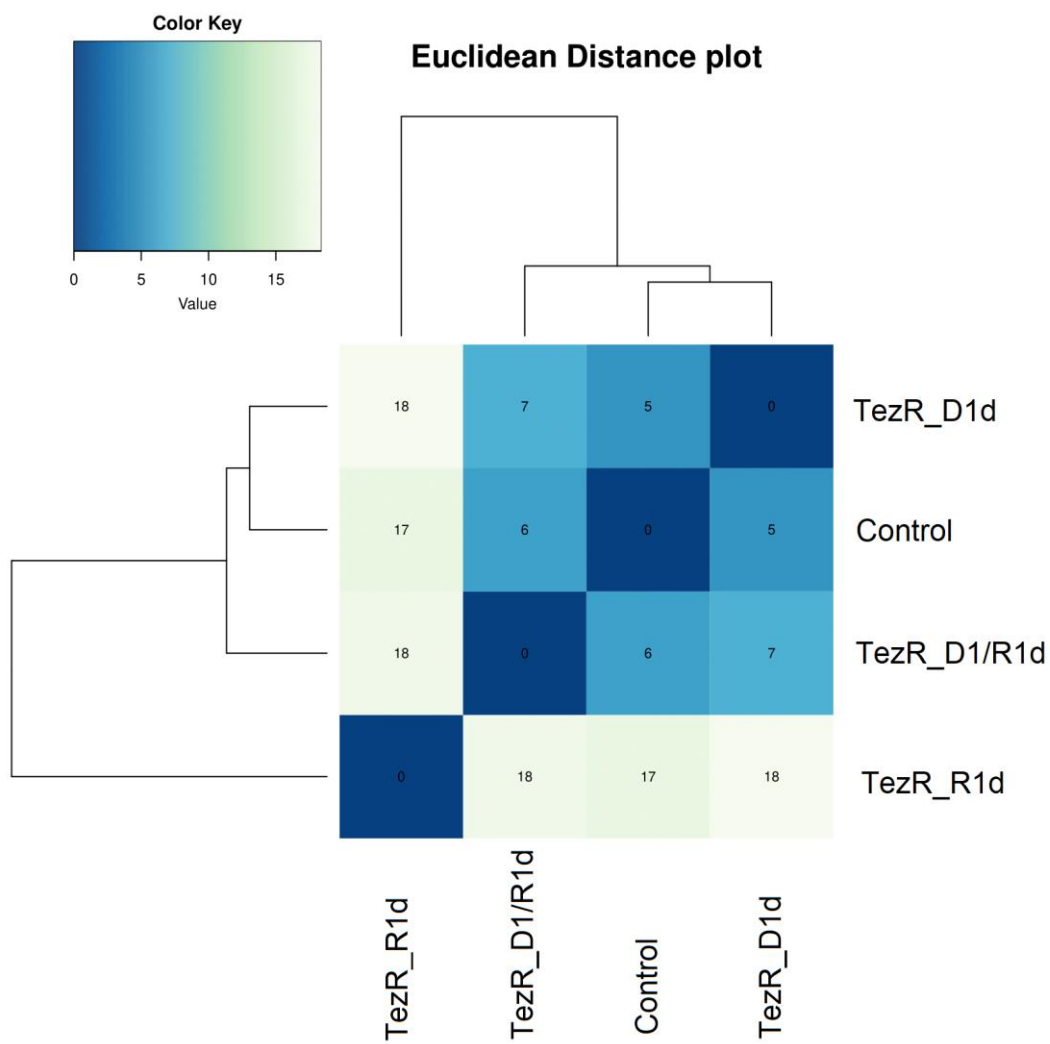
161 Next, we compared the results from each probe and analyzed the genes whose expressions were
162 significantly altered (upregulated or downregulated) following the removal of different TezRs (Fig.
163 2C to D, Supplementary table S1). We identified 128, 150, and 93 differentially expressed proteins
164 (DEPs) in *S. aureus* when compared to TezR_D1^d/control, TezR_R1^d/control, and

165 TezR_D1/R1^d/control, respectively ($|\log_2\text{-fold change}| > 0.5$ and $p\text{-value} < 0.05$). Among the
166 DEPs, 55 proteins were upregulated, and 73 proteins were downregulated in *S.aureus* TezR_D1^d
167 compared to those in the TezR_D1^d/control (Fig. 2C). Among the DEPs in *S.aureus* TezR_R1^d,
168 137 upregulated and 13 downregulated proteins are found compared to those in the
169 TezR_R1^d/control (Fig. 2D). Additionally, 62 upregulated proteins and 31 downregulated proteins
170 are detected in TezR_D1/R1^d/control compared to those in the TezR_D1/R1^d/control. A minute
171 overlap in differentially expressed transcripts were detected in bacteria after the removal of
172 different TezRs. This non-redundancy signifies the individual regulatory roles of TezRs. These
173 data evidently highlight the complex responses triggered by the loss of both primary DNA- and
174 RNA-based TezRs, which cannot be justified by summing up the effects of individual TezRs
175 losses (Fig. 2E). The only gene expression which significantly altered due to the loss of any of
176 the primary TezRs was SA0532 encoding a *Staphylococcus*-specific hypothetical protein (41).
177 Interestingly, following the loss of DNA-based TezRs alone or in combination with RNA-based
178 TezRs, upregulation of proteins associated with type VII secretion system was observed (42, 43).



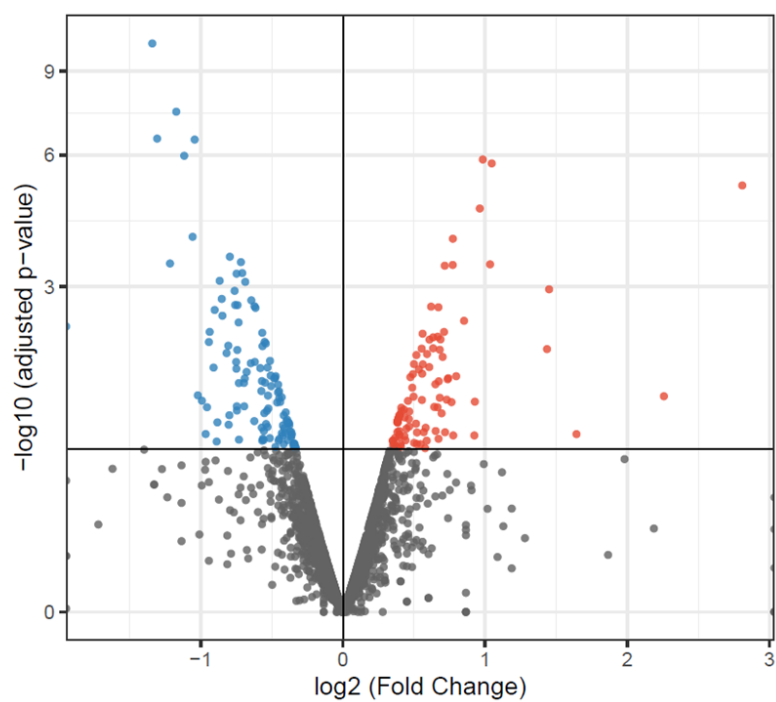
179

180 A



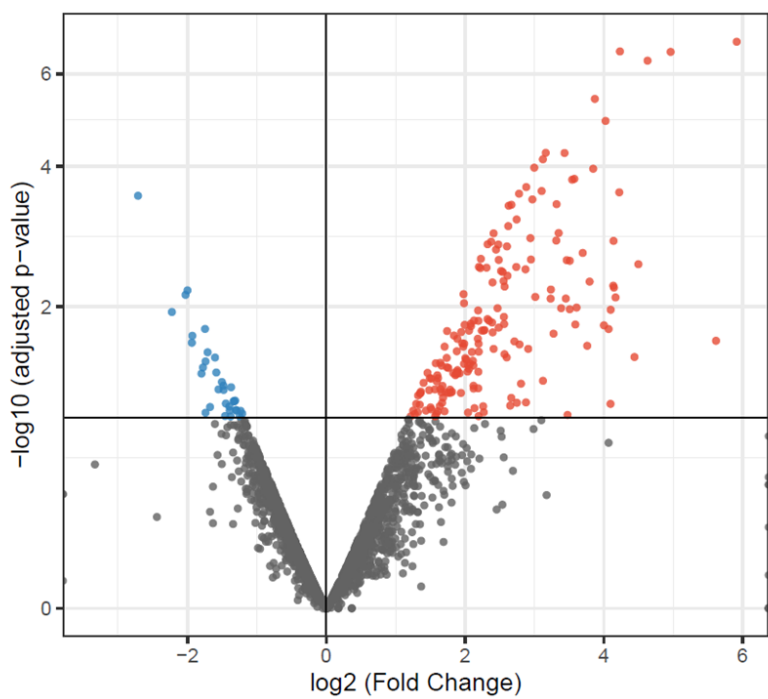
181

182 B



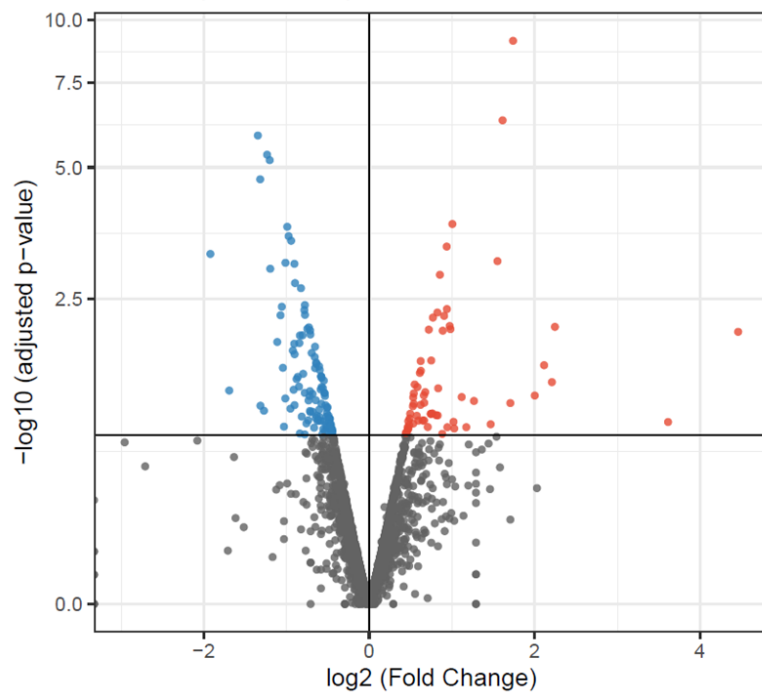
183

184 C



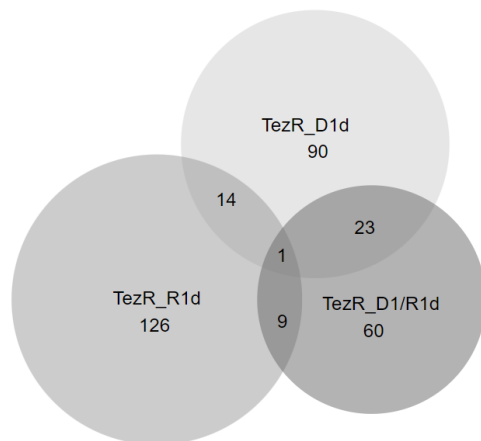
185

186 D



187

188 E



189

190 F

191 Figure 2. Transcriptome analysis of *S. aureus* following the removal of primary TezRs

192

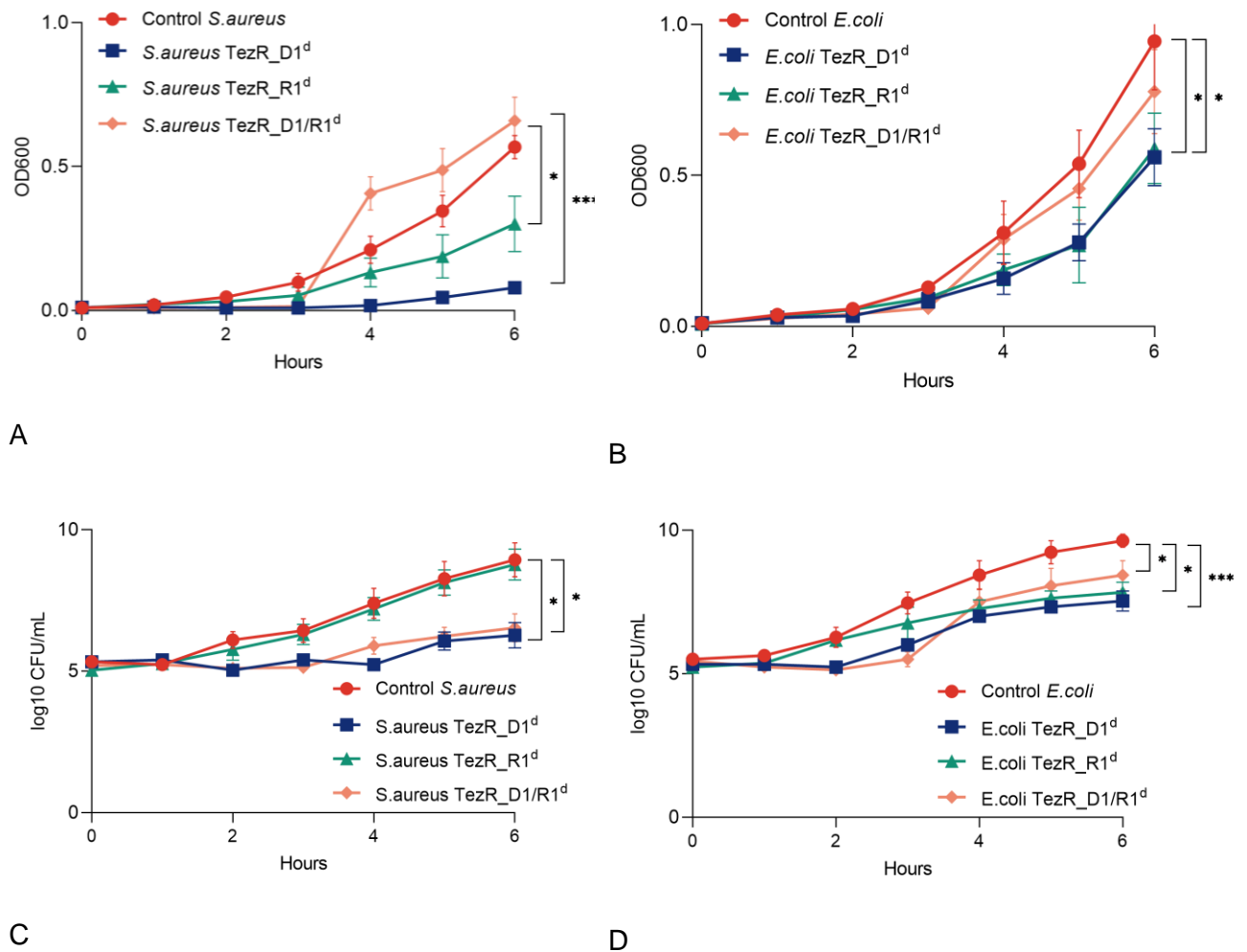
193 (A) PCA plot (B) Heatmap of Euclidean distance (C to E) Volcano plots highlighting the genes
194 that are differentially expressed (\log_2 fold > 0.5 change plotted against the $-\log_{10}$ P-value). The
195 results demonstrate the altered expression levels of the genes following primary TezRs loss (F)
196 the overlap and unique DEPs in each group using Venn diagram

197

198 **TezRs affect microbial growth**

199 Stationary phase *S. aureus* VT209 and *E. coli* ATCC 25922 were left untreated or pretreated with
200 nucleases to remove primary TezRs, after which they were diluted in fresh medium and allowed

201 to grow. OD600 and CFU were measured hourly during the first 6 h of incubation. Growth curves
202 are presented as OD600 values (Fig. 2A, B) or bacterial counts (Fig. 2C, D) as a function of time.



203

204 **Figure 3.** Role of TezRs in the regulation of bacterial growth.

205 Growth comparison of control bacteria and bacteria lacking TezR_D1 (*S. aureus* TezR_D1^d, *E.*
206 *coli* TezR_D1^d), TezR_R1 (*S. aureus* TezR_R1^d, *E. coli* TezR_R1^d) or TezR_D1 and TezR_R1
207 (*S. aureus* TezR_D1/R1^d, *E. coli* TezR_D1/R1^d). (A, B) Bacterial growth measured as OD600
208 over time in (A) *S. aureus* and (B) *E. coli*. (C, D) Bacterial growth measured as bacterial counts
209 (log₁₀ CFU/mL) in (C) *S. aureus* and (D) *E. coli*. Values representing the mean ± SD were
210 normalized to the initial OD600 value. *p < 0.05, ***p < 0.001.

211

212 Removal of primary TezRs retarded bacterial growth in both *S. aureus* and *E. coli* compared with
213 untreated bacteria as measured by OD600 (p < 0.001 and p < 0.05, respectively) and CFU. While
214 the lag phase was 3-h longer for treated *S. aureus*, it was similar between untreated and treated
215 *E. coli*; although the latter exhibited retarded growth by the end of the observation period. At that

216 point, CFU/mL of *S. aureus* TezR_D1^d and *E. coli* TezR_D1^d were lower by 2.6 log₁₀ ($p < 0.05$)
217 and 2.1 log₁₀ ($p < 0.001$) compared with control bacteria.

218 Loss of TezR_R1 in *S. aureus* inhibited bacterial growth, as indicated by OD600 values ($p < 0.05$),
219 but it did not affect bacterial counts. Such a discrepancy points to dysregulation of *S. aureus*
220 TezR_R1^d and can be explained by reduced production of extracellular matrix. A similar effect on
221 growth was observed in *E. coli* following the removal of TezR_R1 (OD600, $p < 0.05$); however,
222 unlike in *S. aureus*, it coincided with reduced CFU ($p < 0.05$).

223 Loss of both primary TezRs in *S. aureus* and *E. coli* extended the lag phase by 3 h; however, this
224 was followed by very rapid growth from 3 to 6 h. Thus, by the end of the observation period,
225 OD600 for *S. aureus* TezR_D1/R1^d was even higher than for control *S. aureus*; while OD600 for
226 *E. coli* TezR_D1/R1^d was only marginally lower than for control *E. coli*. Surprisingly, bacterial
227 counts of *S. aureus* TezR_D1/R1^d and *E. coli* TezR_D1/R1^d were lower throughout the
228 observation period, amounting to 2.4 log₁₀ CFU/mL and 1.2 log₁₀ CFU/mL fewer counts
229 compared with control bacteria after 6 h ($p < 0.05$). Cell size was also reduced at this time point
230 (Supplementary Table 1).

231 The discrepancy between elevated OD600 levels along with delayed bacterial growth and a
232 reduced cell size can be explained by the production of more extracellular matrix. Given similar
233 OD600 values at the end of the observation period between control bacteria and those lacking
234 TezR_D1/R1, we named the latter “drunk cells”.

235 Based on these data we conclude that primary TezRs play a critical regulatory role in bacterial
236 growth by affecting multiple biosynthetic pathways.

237 **Biofilm growth and cell size are regulated by TezRs**

238 We next investigated how TezRs affected biofilm morphology of *B. pumilus* VT1200 grown on
239 agar plates. To analyze the role of primary TezRs, *B. pumilus* were pretreated with nucleases and
240 then inoculated and grown on regular agar medium. To study the role of secondary TezRs, growth
241 of *B. pumilus* was evaluated on medium supplemented with different nucleases. We also
242 established that RNase A used in this study was not internalized by the bacteria under these
243 experimental conditions (Supplementary Fig. 1).

244

245 Biofilms of control *B. pumilus* had a circular shape (Fig. 4A) with smooth margins; whereas those
246 formed by *B. pumilus* TezR_D1^d (Fig. 4B) and *B. pumilus* TezR_R1^d (Fig. 4C) develop blebbing,
247 and those of *B. pumilus* TezR_D1/R1^d exhibited filamentous (filiform) margins (Fig. 4D).

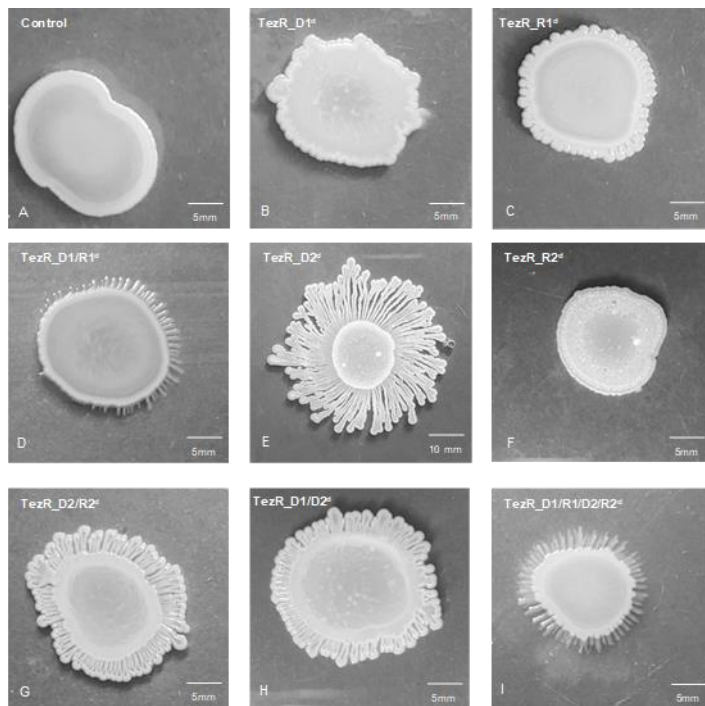
248 *B. pumilus* TezR_D2^d biofilms were characterized by increased swarming motility and formation
249 of significantly larger colonies ($p < 0.001$) with distinct phenotype and dendritic patterns (Fig. 4E);
250 whereas *B. pumilus* TezR_R2^d biofilms had the same size as control *B. pumilus*, but irregular
251 margins and wrinkled surface (Fig. 4F, Supplementary Table 2).

252 Interestingly, the combined removal of other TezRs along with loss of TezR_D2 led to a striking
253 difference compared to the large biofilms formed by *B. pumilus* TezR_D2^d. The biofilms of both
254 *B. pumilus* TezR_D2/R2^d and TezR_D1/D2^d were characterized by a structurally complex,
255 densely branched morphology, but the dendrites were not so profound and the biofilm was not so
256 spread out as in the case of *B. pumilus* TezR_D2^d. The morphology of biofilms formed by bacteria
257 devoid of both primary and secondary TezRs such as *B. pumilus* TezR_D1/R1/D2/R2^d was very
258 similar to that of *B. pumilus* TezR_D1/R1^d, with filamentous (filiform) margins but similar size as
259 control *B. pumilus*.

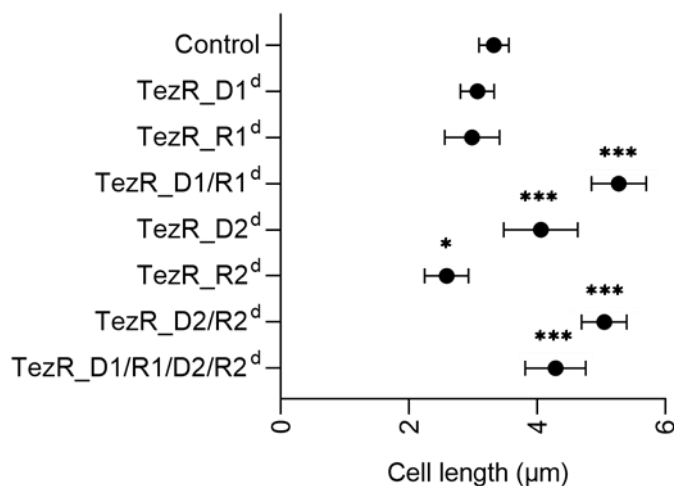
260 In these experiments, nucleases added to the solid nutrient medium with the aim of removing
261 secondary TezRs could potentially affect also cell surface-bound primary TezRs. However, a
262 comparison of the morphology of biofilms formed by *B. pumilus* TezR_D1^d with those of *B.*
263 *pumilus* TezR_D2^d and *B. pumilus* TezR_D1/D2^d (Fig. 4B, E, H) revealed clear differences,
264 meaning that nucleases added to the agar did not alter primary TezRs, at least not in the same
265 way as direct nuclease treatment did.

266 Moreover, the different size of biofilms formed by *B. pumilus* TezR_D2^d vs. *B. pumilus*
267 TezR_D1/D2^d excludes the possibility that the increased colony size of the former resulted from
268 greater swarming motility due to loss of extracellular DNA and decreased extracellular
269 polysaccharide viscosity, because extracellular DNA was eliminated also in the latter (44).
270 Collectively, these data allow us to conclude that different TezRs play an individual regulatory role
271 in biofilm morphology.

272 Next, we found that loss of TezRs had divergent effects on bacterial size. The combined removal
273 of primary TezRs, or secondary TezR_D2 alone or in combination with other TezRs, resulted in
274 significantly increased cell sizes ($p < 0.001$). In comparison, individual loss of secondary
275 TezR_R2s decreased the size of *B. pumilus* cells ($p < 0.05$). Further experiments could not
276 confirm an association between cell size alteration and sporulation triggered by TezRs removal.
277 Possibly, the observed greater mean cell length could result from incomplete cell division and
278 elongation triggered by TezRs destruction (45).



279



280

281 J.

282

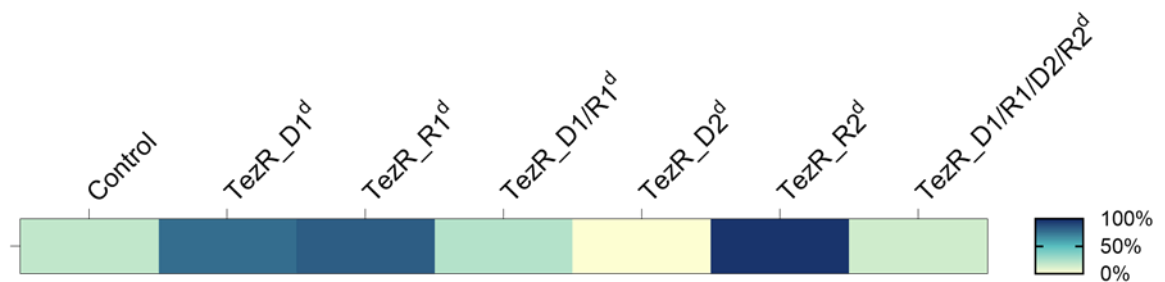
283 **Figure 4.** TezRs regulate biofilm morphology and cell size.

284 Morphology of nuclease-treated or untreated 72-h-old biofilms. (A) Control *B. pumilus*. (B) *B.*
 285 *pumilus* TezR_D1^d. (C) *B. pumilus* TezR_R1^d. (D) *B. pumilus* TezR_D1/R1^d. (E) *B. pumilus*
 286 TezR_D2^d. (F) *B. pumilus* TezR_R2^d. (G) *B. pumilus* TezR_D2/R2^d. (H) *B. pumilus* TezR_D1/D2^d.
 287 (I) *B. pumilus* TezR_D1/R1/D2/R2^d. Scale bars indicate 5 or 10 mm. Representative images of
 288 three independent experiments are shown. (J). Cell length of bacteria grown on solid medium
 289 (μm). *p < 0.05, ***p < 0.001. Data represent the mean ± SD from three independent experiments.

290

291 **TezRs modulate sporulation**

292 Given the significant alterations of biofilm morphology and transcriptome following TezRs loss,
293 we sought evidence for their biological relevance in sporulation. We found that loss of TezR_D1,
294 TezR_R1, and particularly TezR_R2 activated sporulation of *B. pumilus* VT1200 (all $p < 0.001$)
295 (Fig. 5, Supplementary Table 3). In contrast, destruction of TezR_D2 completely repressed
296 sporulation ($p = 0.007$) (Supplementary Table 3).



297

298 **Figure 5.** TezRs regulate sporulation.

299 Heat map of sporulation intensity in cells with altered TezRs under normal conditions. Each cell
300 indicates control *B. pumilus* or *B. pumilus* lacking TezRs. Color-coding indicates the ratio of
301 spores to the total number of cells: white (0% sporulation), dark blue (100% sporulation).

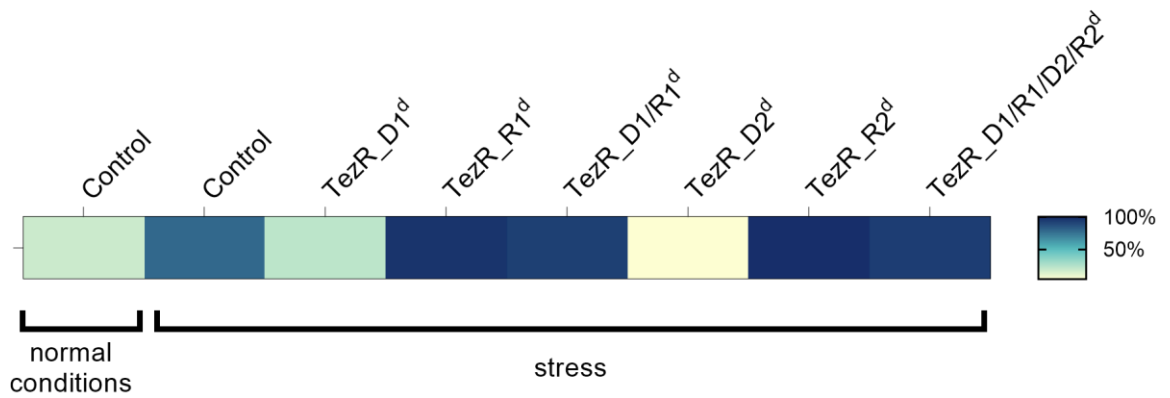
302

303 Notably, sporulation was not affected in “drunk cells” lacking TezR_D1/R1, but was increased if
304 either TezR_D1 or TezR_R1 were removed. This finding highlights the complex web of pathways
305 dictating the responses of “drunk cells”, which do not simply reflect the additive effect of removing
306 individual primary TezRs. Moreover, the result points to the various roles of TezRs in regulating
307 bacterial sporulation.

308 **Role of TezRs in the regulation of stress responses**

309 We next tested whether TezRs regulated also stress responses. The general stress response of
310 control *B. pumilus* VT1200 manifested as increased sporulation (Fig. 6). Removal of TezR_R1 or
311 TezR_R2 alone, or in combination with any other TezRs, upregulated the stress response and
312 stimulated sporulation. Interestingly though, loss of TezR_D1 or TezR_D2 had the opposite effect
313 ($p < 0.001$) (Supplementary Table 4). Hence, loss of TezR_D2 inhibited sporulation under both
314 normal and stress conditions, confirming its implication in regulating the cell stress response.

315



316

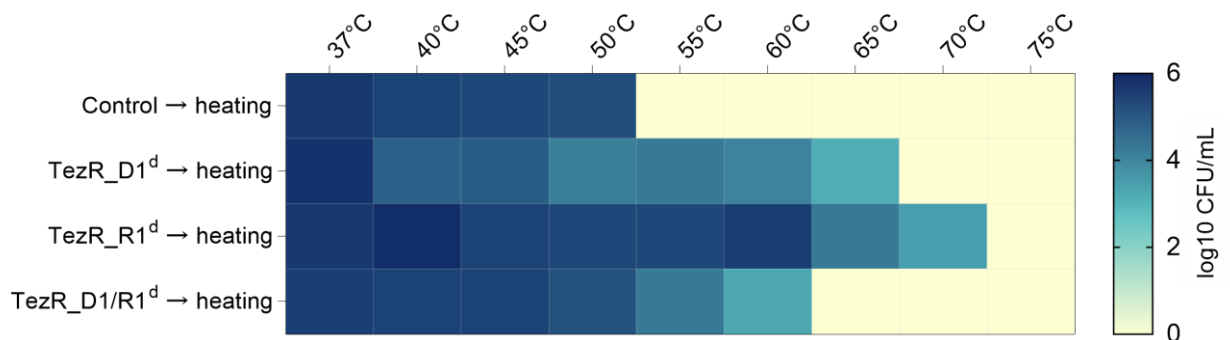
317 **Figure 6.** TezRs regulate sporulation under stress.

318 Heat map of sporulation intensity in *B. pumilus* with altered TezRs under stress conditions. Each
 319 cell indicates control *B. pumilus* or *B. pumilus* lacking TezRs under stress conditions. Color-coding
 320 indicates the ratio of spores to the total number of cells: white (0% sporulation), dark blue (100%
 321 sporulation).

322

323 **TezRs removal results in increased temperature tolerance**

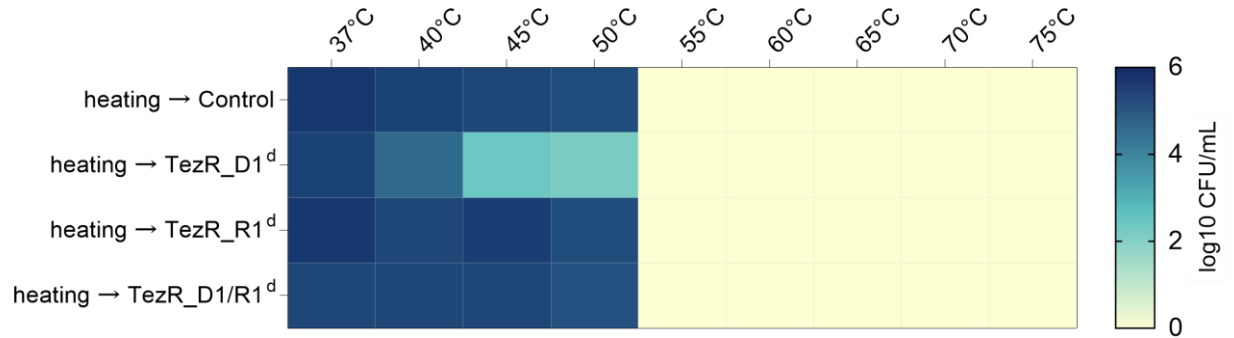
324 Assessment of whether TezRs regulated bacterial thermotolerance revealed that control *S.*
 325 *aureus* VT209 exhibited maximum tolerance at up to 50 °C, whereas *S. aureus* lacking primary
 326 TezRs could survive at even higher temperatures. Specifically, *S. aureus* TezR_D1^Δ survived at
 327 up to 65 °C, *S. aureus* TezR_R1^Δ at up to 70 °C, and *S. aureus* TezR_D1/R1^Δ at up to 60 °C (Fig.
 328 7A).



329

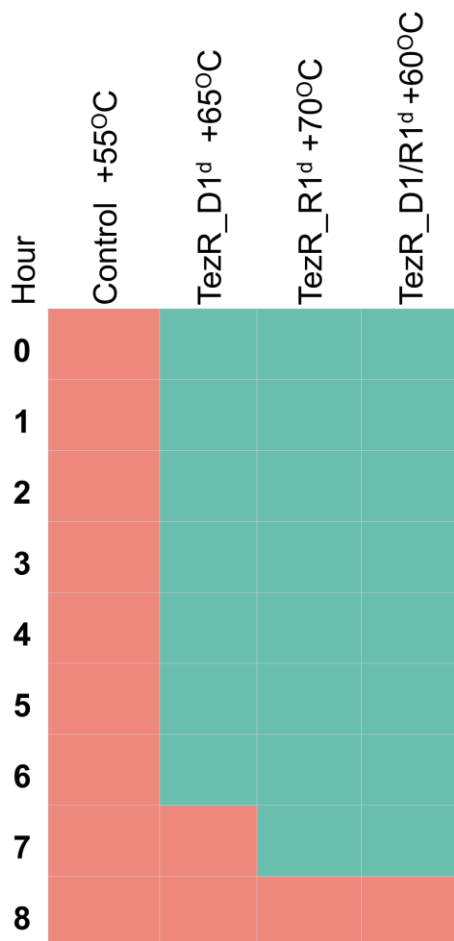
330 A.

331



332

333 B.



334

335 C

336 **Figure 7.** Role of TezRs in survival at the elevated temperature.

337 (A) Heat map summarizing the effect of primary TezRs removal on survival of a *S. aureus* culture

338 heated for 10 min at different temperatures. The color intensity represents the average log₁₀

339 CFU/mL, from white (minimal) to blue (maximum). Values represent the average of three
340 independent experiments. (B) Heat map summarizing the effect of primary TezRs removal on
341 survival after heating of a *S. aureus* culture at different temperatures for 10 min. The color intensity
342 represents the average log₁₀ CFU/mL, from white (minimal) to blue (maximum). Values represent
343 the average of three independent experiments. (C) Heat map representing the time required for
344 the enhanced temperature tolerance of *S. aureus* to disappear in control, TezR_D1^d (65 °C),
345 TezR_R1^d (70 °C), and TezR_D1/R1^d (60 °C) cells. Green squares denote bacterial growth
346 following heating and indicate enhanced temperature survival. Red squares denote lack of
347 bacterial growth following heating and indicate no change in temperature tolerance. Values
348 represent the average of three independent experiments.

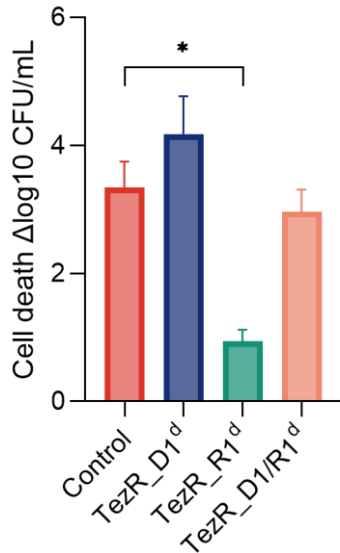
349 We sought to discern whether the observed enhanced temperature survival was attributable to
350 transcriptome-level responses triggered by TezRs removal, or to the direct role of TezRs in
351 sensing and regulation of temperature changes. To this end, we incubated control *S. aureus* at
352 different temperatures and removed primary TezRs right after heating to trigger transcriptionally-
353 induced alterations. Loss of primary TezRs after the heating step did not improve temperature
354 tolerance (Fig. 7B). This result demonstrated that the response of bacteria to higher temperatures
355 was regulated by primary TezRs and depended on their presence at the time of heating, rather
356 than being induced by their loss.

357 Next, we evaluated how much time was required for bacteria, which became resistant to heating
358 after primary TezRs removal, to recover normal temperature sensing. This information could be
359 used as a surrogate marker of the time required for restoration of functionally active cell surface-
360 bound TezRs. *S. aureus* TezR_D1^d, TezR_R1^d, and TezR_D1/R1^d were inoculated in culture
361 broth and grown at the maximum temperature tolerated by bacteria following each specific TezR
362 destruction (65, 70, and 60°C, respectively) (Fig. 7C). Control *S. aureus* were processed in the
363 same way and heated at 55 °C as their next-to-lowest non-tolerable temperature. Each hour after
364 heating, bacteria were inoculated in fresh LB broth to assess the presence or absence of growth
365 after 24 h at 37 °C. Growth meant that bacteria still possessed enhanced temperature survival
366 and the corresponding time indicated no restoration of functionally active primary TezRs. In turn,
367 absence of growth could mean that functionally active primary TezRs were restored and bacteria
368 could normally sense and respond to the higher temperature. After TezRs removal, it took from 7
369 to 8 h for *S. aureus* to restore functionally active primary TezRs and normal temperature tolerance
370 (Fig. 7C). Taken together, these data demonstrate that TezRs participate in temperature sensing
371 and the regulation of the corresponding response.

372 **TezRs regulate UV resistance**

373 To determine whether TezRs participated in UV resistance, we exposed cells to UV light. Loss of
374 TezR_D1 and TezR_D1/R1 had no statistically significant effect on the survival of *S. aureus*

375 following UV irradiation compared to control bacteria (Fig. 8). Notably, loss of TezR_R1 protected
376 bacteria from UV-induced death, and resulted in 2.4 log₁₀ CFU/mL higher viable counts
377 compared to control *S. aureus* following UV irradiation ($p = 0.002$). These data suggest that TezRs
378 participate in sensing and response to UV irradiation.



379

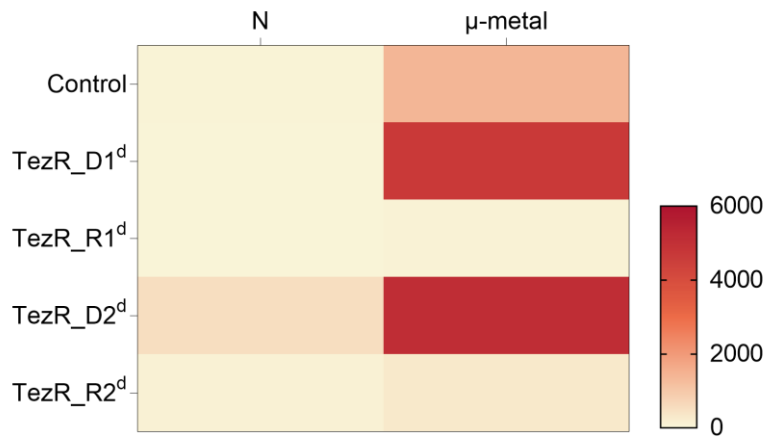
380 **Figure 8.** Role of primary TezRs in resistance of *S. aureus* to UV exposure.

381 Comparison of live bacteria measured as bacterial counts (log₁₀ CFU/mL) before and after UV
382 exposure. Data represent the mean ± SD of three independent experiments. $p < 0.05$ was
383 considered significant.

384

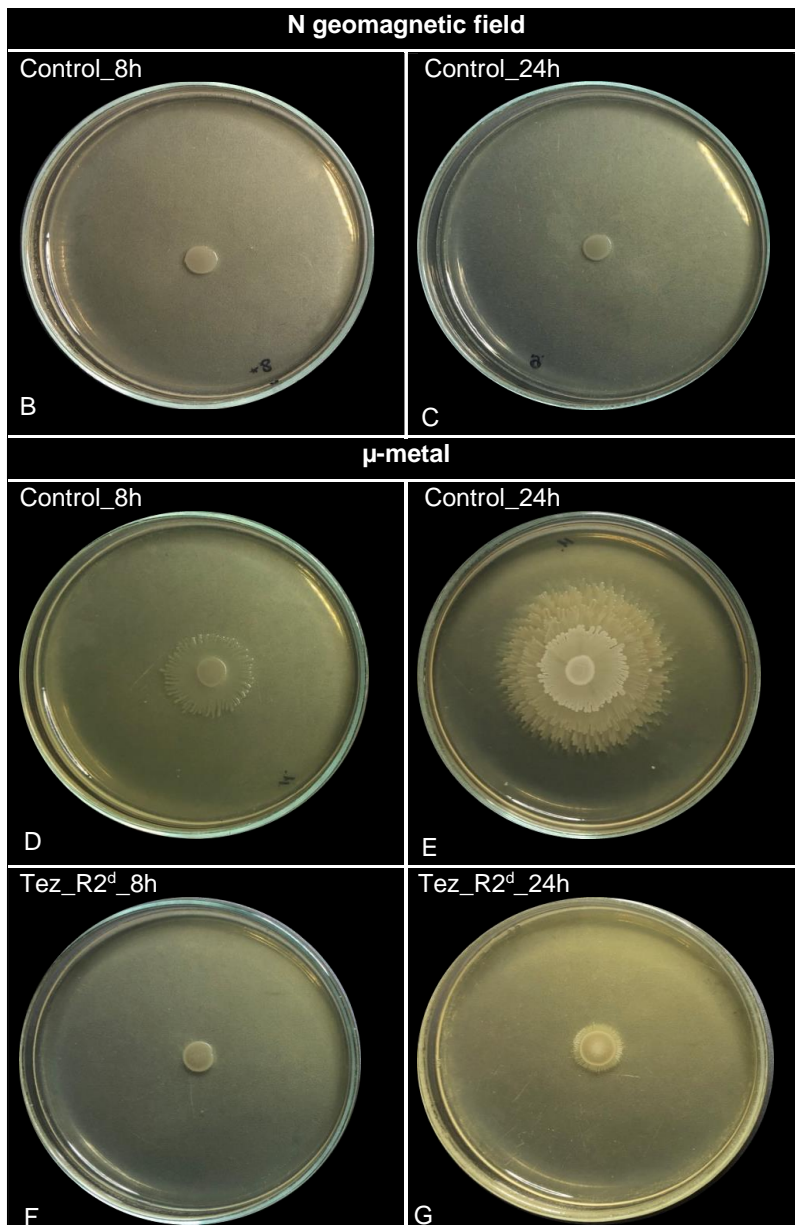
385 **Magnetoreception relies on TezRs**

386 The magnetoreceptive function of TezRs was assessed by morphological changes at
387 a macroscopic scale in agar-grown *B. pumilus* VT1200 biofilms following inhibition of the
388 geomagnetic field (Fig. 9A, B).



389

390 A



391

392 B

393 **Figure 9.** Role of TezRs in magnetoreception of *B. pumilus*.

394 (A) Heat map representing the effect of TezRs loss on the size of the biofilm area under normal
395 (N) and inhibited geomagnetic (μ -metal) fields after 24 h of growth. The size of the biofilm is
396 represented by a color scale, from white (minimum) to red (maximum). (B–G) Dynamic changes
397 to biofilm morphology in cells exposed to normal or inhibited geomagnetic field during 8 and 24 h
398 of growth: (B, C) control *B. pumilus* under normal magnetic field; (D, E) control *B. pumilus* under
399 inhibited (μ -metal) geomagnetic field; and (F, G) *B. pumilus* TezR_R2^d under inhibited (μ -metal)
400 geomagnetic field.

401 Inhibition of the geomagnetic field promoted growth of control *B. pumilus* biofilms compared to
402 cells grown under unaltered magnetic conditions (Fig. 9A, E). Loss of TezR_D1 or TezR_D2
403 stimulated bacterial growth in response to inhibition of the geomagnetic field across the entire
404 plate (Fig. 9A). Instead, biofilms formed by *B. pumilus* following loss of TezR_R1 or TezR_R2
405 presented a strikingly diminished response to inhibition of the geomagnetic field. When compared
406 with biofilms formed by control *B. pumilus*, those formed by *B. pumilus* TezR_R1^d or TezR_R2^d
407 grown in a μ -metal cylinder for 24 h displayed only a negligible increase in size (Fig. 9A). However,
408 they still exhibited minor changes in morphology compared with their counterparts grown under
409 unaltered magnetic conditions (Fig. 9C, G).

410 To further elucidate the detailed role of RNA-based TezRs in sensing and responding to the
411 geomagnetic field, we analyzed the time it took for morphological differences between control and
412 *B. pumilus* TezR_R2^d biofilms placed in a μ -metal cylinder to occur. We found that already after
413 8 h, biofilms of control *B. pumilus* cultivated under inhibited geomagnetic field (Fig. 9D) presented
414 an altered morphology with an increased size and irregular edge compared with those grown
415 under normal conditions (Fig. 9B). In contrast, the morphology of *B. pumilus* TezR_R2^d biofilms
416 was identical in the absence (Fig. 9F) or presence (Fig. 9B) of a regular geomagnetic field. These
417 results showed that the alterations of biofilm morphology observed in *B. pumilus* TezR_R2^d in the
418 inhibited geomagnetic field (Fig. 9G) occurred within 8–24 h. Together with our data pointing to
419 the need for *S. aureus* for 8 h to restore normal temperature tolerance, these results add another
420 line of evidence that bacteria started responding to geomagnetic field only after TezRs have been
421 restored. Overall, RNA-based TezRs might be implicated in sensing and regulation of cell
422 response to the geomagnetic field. These findings also highlight the complex web of interactions
423 between different TezRs, as some of them adapt their regulatory role to the presence or absence
424 of other TezRs.

425 **TezRs are required by bacteria for light sensing**

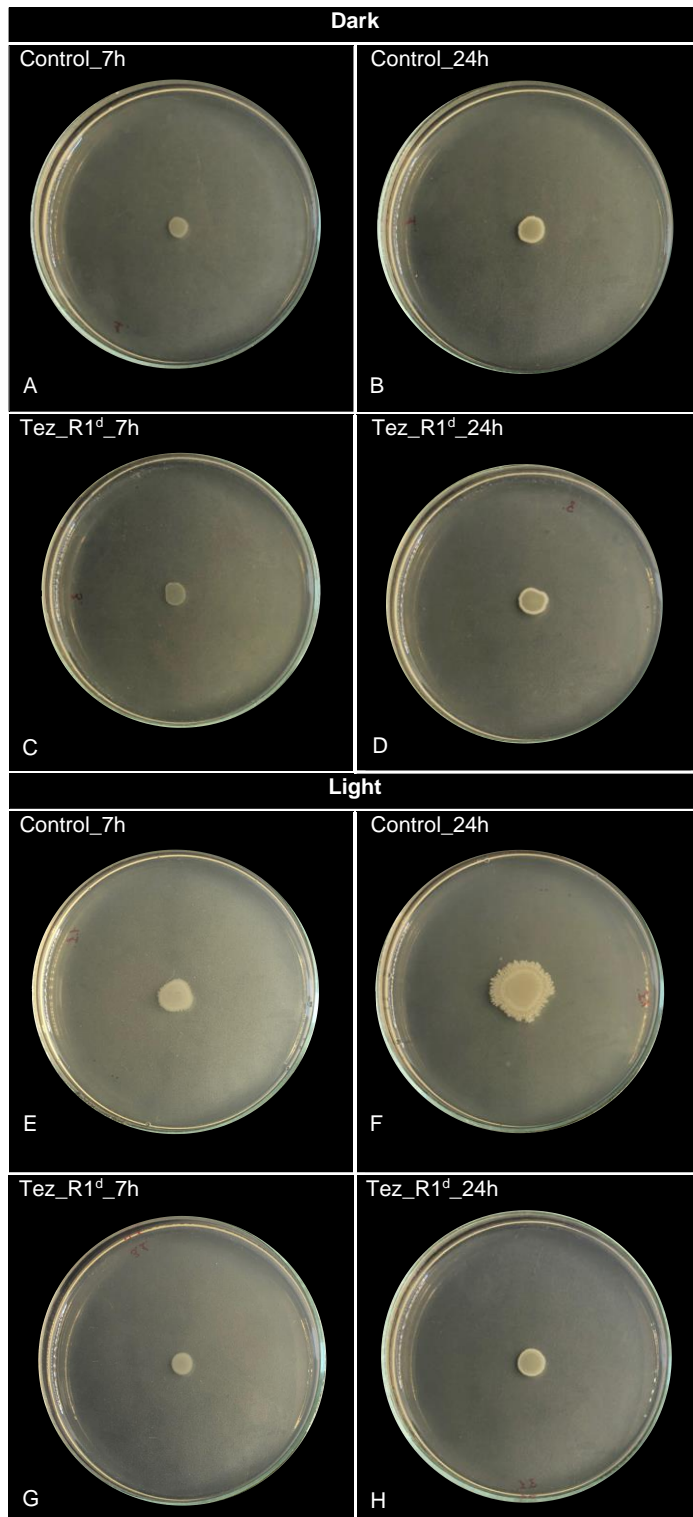
426 Given the broad regulatory functions of TezRs in mediating the interaction between bacteria and
427 the surrounding environment, we sought evidence for their biological relevance in sensing visible

428 light. We analyzed differences in morphology of biofilms formed by control *B. pumilus* and *B.*
429 *pumilus* following TezRs removal grown under light vs. dark conditions. Bacterial biofilms formed
430 by either control *B. pumilus* or those lacking TezRs, except TezR_D2, responded to light by
431 forming large biofilms with filamentous (filiform) margins (Fig. 10, Supplementary Fig. 2).

432 In contrast, *B. pumilus* TezR_D2^d grown under light exhibited reduced biofilm size compared to
433 those grown under dark conditions (Supplementary Fig. 2). Strikingly, 24-h-old biofilms formed by
434 *B. pumilus* TezR_R1^d and TezR_R2^d grown in the light presented altered margins, but their
435 growth was contained compared with that of control *B. pumilus*.

436 As in the case of magnetoreception, we hypothesized that the reason for the observed phenotype
437 was that *B. pumilus* TezR_R1^d and *B. pumilus* TezR_R2^d started responding to light only after 7
438 h, when either their RNA-based TezRs were restored or when the cell's normal response was
439 restored after TezR destruction. Therefore, we analyzed the morphology of 7-h-old biofilms grown
440 under light conditions (Fig. 10). By that time, biofilms of control *B. pumilus* already had an altered
441 morphology compared with those grown in the dark. In contrast, the morphology of *B. pumilus*
442 TezR_R1^d was identical irrespective of illumination conditions. Accordingly, changes to biofilm
443 morphology of *B. pumilus* TezR_R1^d occurred within 7–24 h of growth in the light, when TezR_R1
444 should have already been restored.

445 Together, the results imply that TezRs are involved in the regulation of microbial light sensing.
446 Specifically, we found a positive association between the ability of bacteria to sense and respond
447 to light, and the presence of RNA-based TezRs.



448

449 **Figure 10.** Role of TezRs in light sensing.

450 (A - D) Images of (A, B) control *B. pumilus* (Control) and (C, D) *B. pumilus* TezR_R1^d (TezR_R1^d)

451 incubated in the dark for 7 h and 24 h. (E - H) Images of (E, F) control *B. pumilus* and (G, H) *B.*

452 *pumilus* TezR_R1^d incubated in the light for 7 h and 24 h.

453

454

455 **TezRs regulate anaerobic survival of aerobes**

456 Intuitively, we hypothesized that TezRs might regulate the bacterial response to a changing gas
457 composition. To test this hypothesis, we used the obligate aerobe *P. putida*, generally known for
458 its inability to perform anaerobic fermentation. Introduction of numerous additional genes, a
459 massive restructuring of its transcriptome, and nutrient supplementation have been proposed as
460 the only means to accommodate anoxic survival of this species (46–49).

461 Control *P. putida* and *P. putida* lacking TezRs were placed on agar and cultivated under anoxic
462 conditions. While control *P. putida*, and *P. putida* deficient in TezR_D1 or TezR_D2 alone, or in
463 combination with loss of RNA-based TezRs, could not grow under anaerobic conditions, loss of
464 only RNA-based TezRs allowed for anaerobic growth of *P. putida* (Fig. 11A, B). *P. putida*
465 TezR_R1^d and TezR_R2^d were characterized by microcolonies crowding (Fig. 11 A, B).

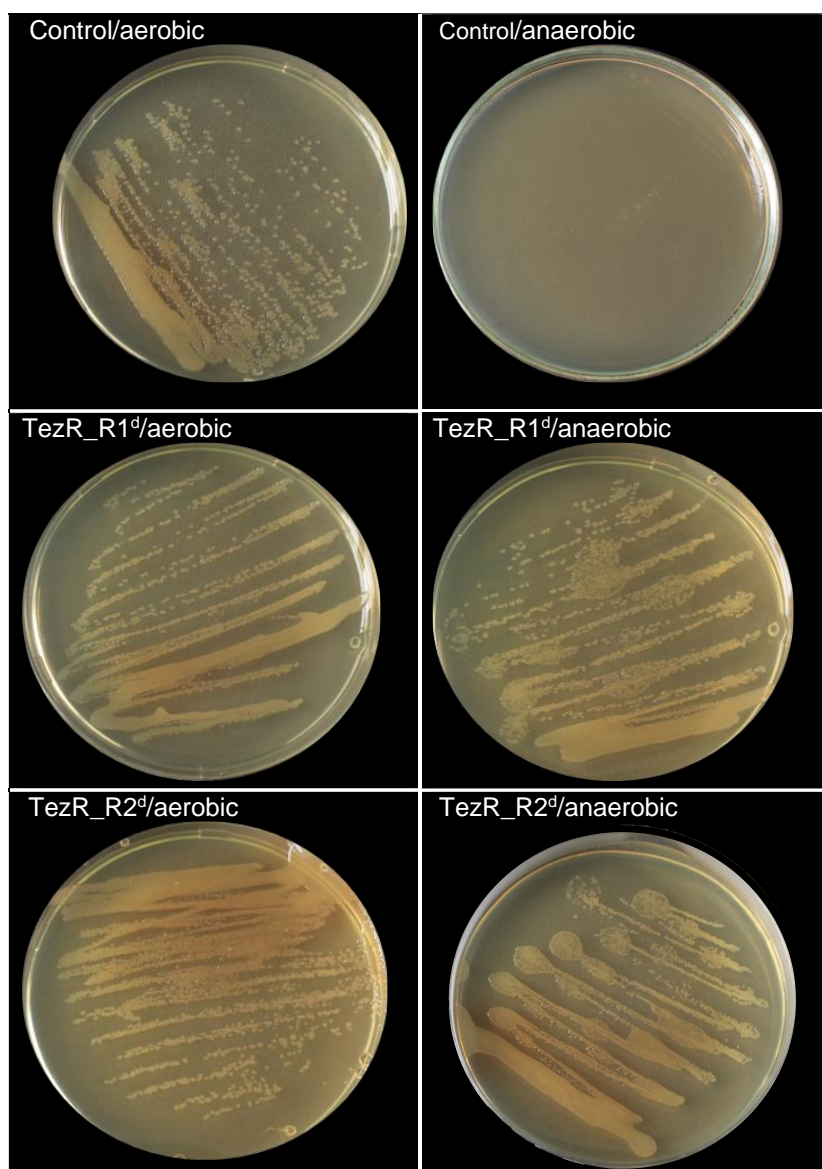
466 We compared the biochemical profile of *P. putida* TezR_R2^d grown in anoxic conditions with
467 control *P. putida* and aerobically grown *P. putida* TezR_R2^d using the VITEK® 2 system (Fig.
468 11C). We observed activation of the urease enzyme in both aerobically and anaerobically grown
469 *P. putida* TezR_R2^d. This enzyme is considered essential for anaerobic fermentation in this
470 species (46). Moreover, when *P. putida* TezR_R2^d were cultivated under anoxic conditions, we
471 noted the activation of some aminopeptidases and glycolytic enzymes known to participate in
472 microbial anaerobic survival in the absence of external electron acceptors such as oxygen (50–
473 53).

474 Collectively, the findings point to a previously unknown sensing and regulatory function of the
475 TRB-receptor system and, in particular, the role of TezR_R1 and TezR_R2 in adaptation to
476 variations in gas composition. Importantly, loss of these TezRs enables obligatory aerobic *P.*
477 *putida* to grow under anoxic conditions.

478

| Probe | Growth of <i>P.putida</i> | |
|------------------------|---------------------------|-----------|
| | Aerobic | Anaerobic |
| Control | + | - |
| Tez_D1 ^d | + | - |
| Tez_R1 ^d | + | + |
| Tez_D1/R1 ^d | + | - |
| Tez_D2 ^d | + | - |
| Tez_R2 ^d | + | + |
| Tez_D1/D2 ^d | + | - |

479 A



480

481

B

| | Control_AERO | TezR_R2d AERO | TezR_R2d ANAERO |
|--------------------------------------|--------------|---------------|-----------------|
| Ala-Phe-Pro-ARYLAMIDASE | + | + | + |
| ADONITOL | + | + | + |
| L-Pyrrolydonyl-ARYLAMIDASE | + | + | + |
| L-ARABITOL | + | + | + |
| D-CELLOBIOSE | + | + | + |
| BETA-GALACTOSIDASE | + | + | + |
| HAla-Phe-Pro-ARYLAMIDASES PRODUCTION | + | + | + |
| BETA-N-ACETYL-GLUCOSAMINIDASE | + | + | + |
| Glutamyl Arylamidase pNA | + | + | + |
| D-GLUCOSE | + | + | + |
| GAMMA-GLUTAMYL-TRANSFERASE | + | + | + |
| FERMENTATION/ GLUCOSE | + | + | + |
| BETA-GLUCOSIDASE | + | + | + |
| D-MALTOSE | + | + | + |
| D-MANNITOL | + | + | + |
| D-MANNOSE | + | + | + |
| BETA-XYLOSIDASE | + | + | + |
| BETA-Alanine arylamidase pNA | + | + | + |
| L-Proline ARYLAMIDASE | + | + | + |
| LIPASE | + | + | + |
| PALATINOSE | + | + | + |
| Tyrosine ARYLAMIDASE | + | + | + |
| UREASE | + | + | + |
| D-SORBITOL | + | + | + |
| SACCHAROSE/SUCROSE | + | + | + |
| D-TAGATOSE | + | + | + |
| D-TREHALOSE | + | + | + |
| CITRATE (SODIUM) | + | + | + |
| MALONATE | + | + | + |
| L-ARABITOL-KETO-D-GLUCONATE | + | + | + |
| L-LACTATE alkalization | + | + | + |
| ALPHA-GLUCOSIDASE | + | + | + |
| SUCCINATE alkalization | + | + | + |
| Beta-N-ACETYL-GALACTOSAMINIDASE | + | + | + |
| ALPHA-GALACTOSIDASE | + | + | + |
| PHOSPHATASE | + | + | + |
| Glycine ARYLAMIDASE | + | + | + |
| ORNITHINE DECARBOXYLASE | + | + | + |
| LYSINE DECARBOXYLASE | + | + | + |
| L-HISTIDINE assimilation | + | + | + |
| COUMARATE | + | + | + |
| BETA-GLUCURONIDASE | + | + | + |
| O/1Tyrosine ARYLAMIDASE RESISTANCE | + | + | + |
| Glu-Gly-Arg-ARYLAMIDASE | + | + | + |
| L-MALATE assimilation | + | + | + |
| ELLMAN | + | + | + |
| L-LACTATE assimilation | + | + | + |

482

483 C

484

485 **Figure 11.** Role of TezRs in growth of *P. putida* under anaerobic conditions.

486 (A) Effect of TezRs loss on the growth of *P. putida* under aerobic and anaerobic conditions.

487 Presence of bacterial growth is marked with a “+” sign, absence of bacterial growth is marked

488 with a “-” sign. Values correspond to representative results of three independent experiments. (B)

489 Growth of control *P. putida*, *P. putida* TezR_R1^d, and *P. putida* TezR_R2^d under aerobic or

490 anaerobic conditions for 24 h. (C) Biochemical profile of control *P. putida* grown under aerobic

491 conditions (Control_aero) and *P. putida* TezR_R2^d cultivated under aerobic (TezR_R2^d_aero)

492 and anaerobic (TezR_R2^d_anaero) conditions in a VITEK® 2 system. Green color denotes

493 positive test reaction results, red color denotes negative results. Values correspond to

494 representative results of three independent experiments.

495 **Bacterial chemotaxis and biofilm dispersal are controlled by TezRs**

496 Bacterial chemotaxis and biofilm dispersal are essential for colonizing various environments,

497 allowing bacteria to escape stress, migrate to a nutritionally richer environment, and efficiently

498 invade a host (54, 55, 56). Although *Bacillus* spp. is believed to rely on transmembrane

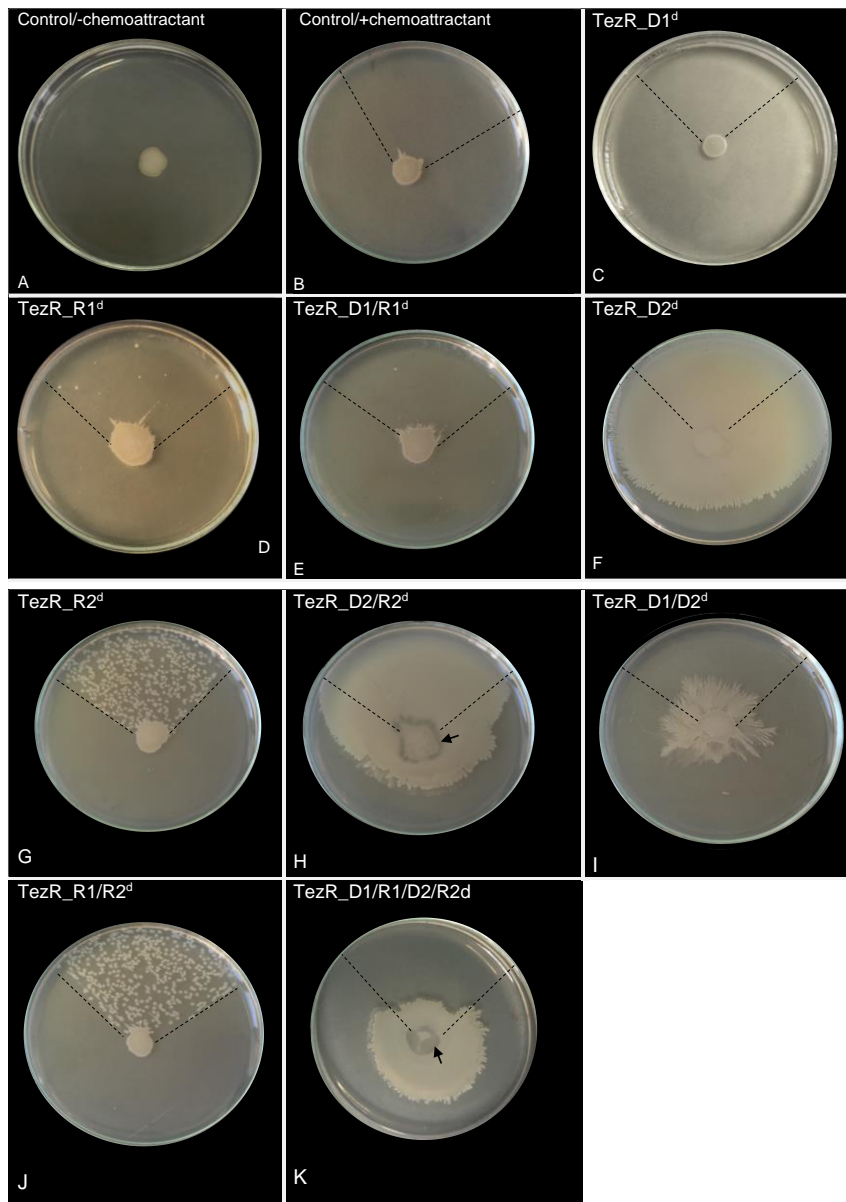
499 chemoreceptors to detect environmental chemical stimuli and a kinase (CheA) and response

500 regulator (CheY) to mediate downstream signals, it remains to be determined how the receptor
501 senses such stimuli (57–59). Moreover, the gene network and signal transduction pathways
502 controlling bacterial dispersal remain largely unexplored.

503 Here, we examined the role of TezRs in bacterial chemotaxis and dispersal in motile *B. pumilus*
504 VT1200.

505 Control *B. pumilus* grew on the agar surface as round biofilms (Fig. 12A); however, addition of
506 human plasma as a chemoattractant, triggered directional migration towards the plasma (Fig.
507 12B). Visual examination of biofilms revealed that *B. pumilus* TezR_D1^d lost their chemotaxis
508 ability, while *B. pumilus* TezR_R1^d triggered biofilm dispersal within the chemoattractant zone
509 (Fig. 12C–E). Biofilms formed by *B. pumilus* TezR_D2^d displayed marked chemotaxis towards
510 plasma along with expanded biofilm growth, which appeared typical for this mutant even in the
511 absence of chemoattractant (Fig. 12F). Loss of TezR_R2 induced marked biofilm dispersal
512 towards the chemoattractant (Fig. 12G) and was accompanied by the formation of multiple
513 separate colonies in the agar zone where plasma was added. Combined elimination of both DNA-
514 and RNA-based secondary TezRs maintained biofilm expansion and chemotaxis behavior (Fig.
515 12H) typical of *B. pumilus* TezR_D2^d; however, the primary community was characterized by
516 zones of active sporulation (Supplementary Fig. 2).

517 Interestingly, combined removal of primary and secondary DNA-based TezRs did not affect
518 chemotaxis (Fig. 12I); however, *B. pumilus* TezR_D1/D2^d displayed geometrical swarming motility
519 patterns with branched biofilm morphology, not observed in any other TezRs mutant of *B. pumilus*.
520 Surprisingly, loss of all primary and secondary TezRs of *B. pumilus* prevented growth towards the
521 chemoattractant, leading instead to negative chemotaxis away from plasma, and appearance of
522 zones of active sporulation (Fig. 12K). These results point to the unique individual sensory and
523 regulatory properties of TezRs in mediating chemotaxis, biofilm morphology, and dispersal.
524 Biofilm dispersal triggered by the removal of TezR_R1 and TezR_R2 in the presence of
525 chemoattractant occurred only in intact DNA-based TezRs. Hence, bacterial interaction with the
526 chemoattractant is regulated by the TRB-receptor system through apparent cooperation between
527 RNA- and DNA-based TezRs, as evidenced by the complex responses triggered by loss of
528 multiple TezRs, and which cannot be accounted for by summing up the effect of individual TezRs
529 losses.



530

531

532

Figure 12. Effect of TezRs on *B. pumilus* chemotaxis to plasma and biofilm dispersal.

533

534

535

536

537

538

539

540

541

542

(A) Control *B. pumilus* with no chemoattractant added. (B) Chemotaxis of control *B. pumilus* towards plasma as chemoattractant. (C) Chemotaxis of *B. pumilus* TezR_D1^d. (D) Biofilm dispersal and chemotaxis of *B. pumilus* TezR_R1^d. (E) Chemotaxis of *B. pumilus* TezR_D1/R1^d. (F, H) Chemotaxis and visibly expanded biofilm growth of *B. pumilus* TezR_D2^d and *B. pumilus* TezR_D2/R2^d. (G, J) Chemotaxis and intense biofilm dispersal of *B. pumilus* TezR_R2^d and *B. pumilus* TezR_R1/R2^d. (I) Chemotaxis of *B. pumilus* TezR_D1/D2^d. (K) Negative chemotaxis of *B. pumilus* TezR_D1/R1/D2/R2^d. Black dotted lines denote the area in which plasma was placed. The black arrow points to zones of active sporulation. A chemotactic response is visualized as a movement of the biofilm away from the center towards the chemoattractant.

542

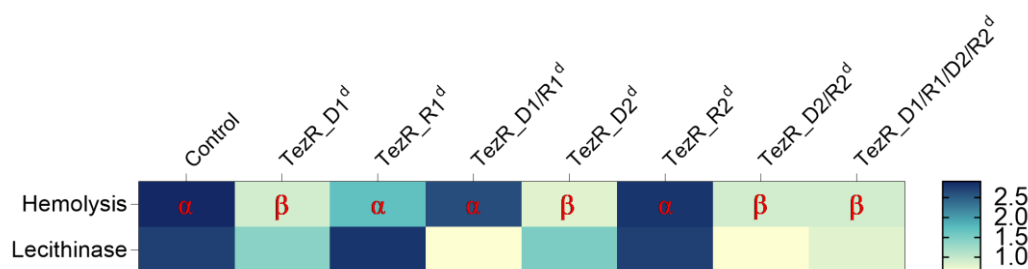
543 **Functional responses induced by loss of TezRs include regulation of bacterial virulence**

544 Membrane-damaging toxins that cause hemolysis or lecithin hydrolysis are critical for *S. aureus*
545 virulence; however, regulation of their functioning remains poorly understood (60). In accordance
546 with the observed pluripotent regulatory role of TezRs, we investigated the effect of TezRs loss
547 on the hemolytic and lecithinase activities of *S. aureus* SA58-1. Loss of TezR_D1 or TezR_D2
548 alone, or in combination with other TezRs, statistically inhibited hemolysis ($p < 0.05$) and triggered
549 the switch from α -hemolysis to β -hemolysis (Fig. 13A), pointing to the activation of genes
550 encoding different hemolysins.

551 A similar pattern was observed regarding the role of TezRs in regulating lecithinase activity (Fig.
552 13A), which was also inhibited following loss of DNA-based TezRs alone or in combination with
553 RNA-based TezRs ($p < 0.05$). In contrast, loss of TezR_R1 or TezR_R2 alone caused no
554 statistically significant alterations of hemolytic and lecithinase activities.

555 To further clarify the role of TezRs in virulence, we used a mouse model of *S. aureus* peritoneal
556 infection. Mice were intraperitoneally challenged with $10.1 \log_{10}$ CFU/mouse containing control
557 *S. aureus*, *S. aureus* TezR_D1^d, *S. aureus* TezR_R1^d or *S. aureus* TezR_D1/R1^d (Fig. 13B–E).
558 All animals exhibited typical signs of acute infection within 12 h, including hypothermia, hunched
559 posture and slightly reduced movement, piloerection, breathing difficulty, narrowed palpebral
560 fissures, trembling, and reduced locomotor activity. Bacterial load was measured in the abdomen,
561 spleen, liver, and kidneys 12 h post infection by aspiration from the abdomen or homogenization
562 of organs, plating on selective *S. aureus* medium, and subsequent identification by microscopy.

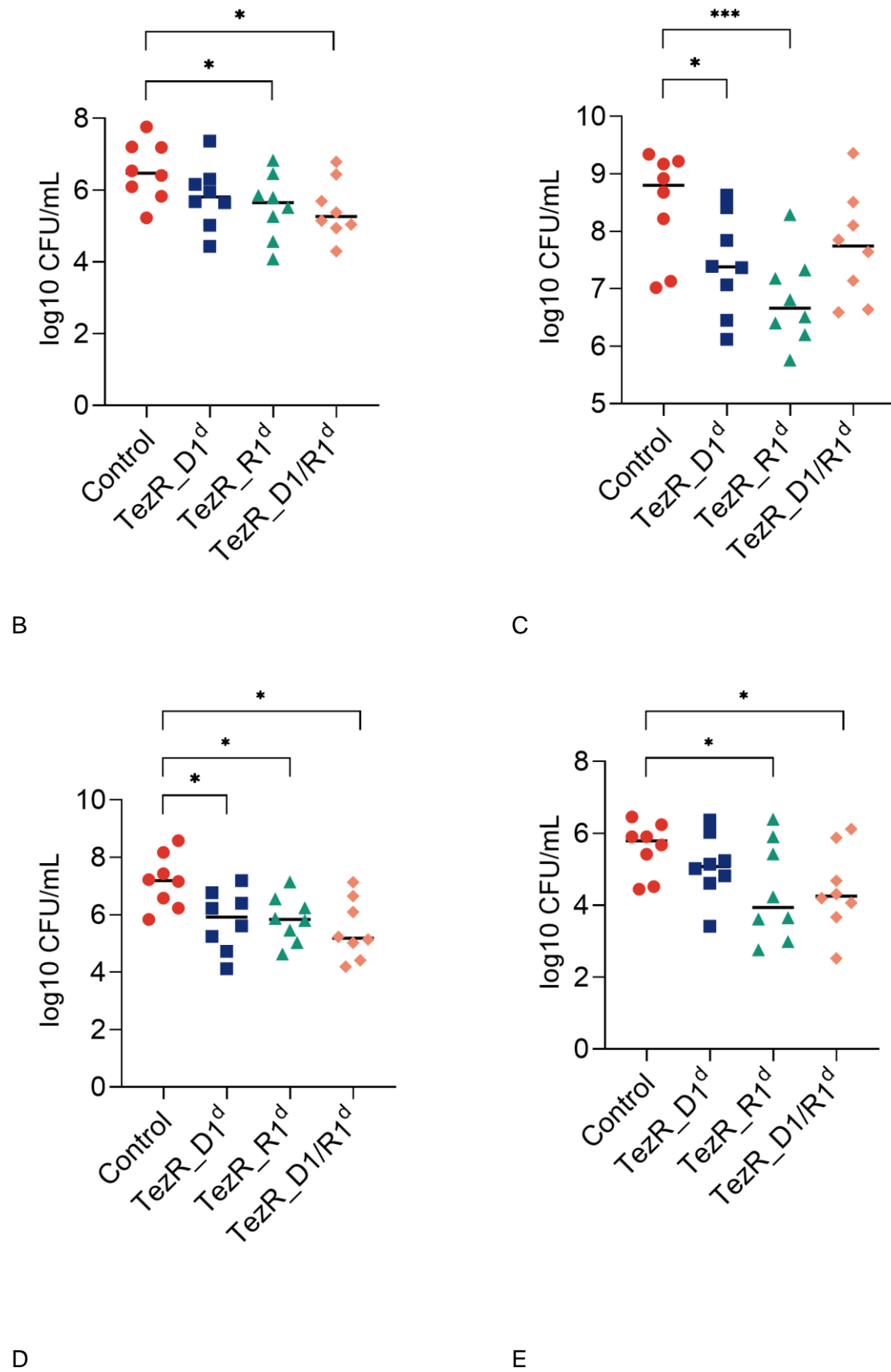
563 Loss of any of the primary TezRs altered the host-parasite relationship, decreasing dissemination
564 of *S. aureus*. The most pronounced decrease was observed in the liver, kidney, and spleen in the
565 group challenged with *S. aureus* TezR_R1^d. Reduction of *S. aureus* dissemination was less clear
566 following infection with *S. aureus* TezR_D1^d or *S. aureus* TezR_D1/R1^d, although it nevertheless
567 resulted in a significant drop in viable counts in some organs. Taken together, these results imply
568 that bacteria disseminated less effectively following loss of TezRs, which can be associated with
569 their higher susceptibility to the host immune response or altered adaptation to the environment.



570

571 A

572



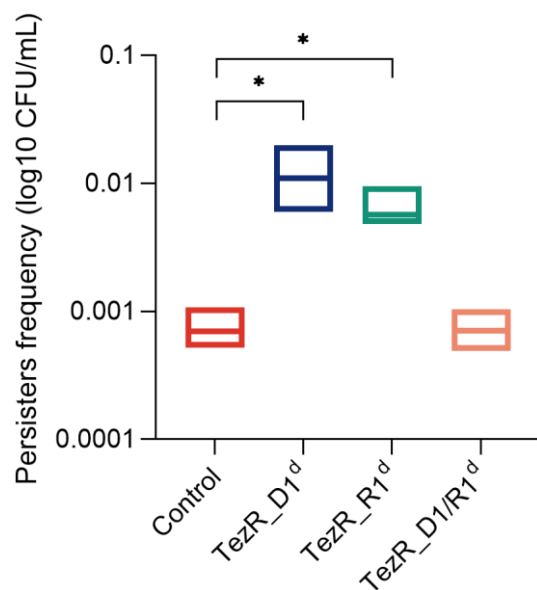
573

574 **Figure 13.** Role of TezRs in virulence.

575 (A) Role of TezRs in the regulation of *S. aureus* hemolysis and lecithinase activities. Hemolytic
576 activity of control *S. aureus* or *S. aureus* lacking TezRs is represented by a clear zone around the
577 colonies on sheep blood agar plates. The presence of α - or β -hemolysis is marked with red letters.
578 Lecithinase activity was analyzed by measuring a white diffuse zone surrounding the colonies.
579 The extent of hemolysis and lecithinase zones (in mm) ranges from white (minimal) to dark blue
580 (maximum). (B–E) Bacterial burden in animals intraperitoneally challenged either with control *S.*
581 *aureus*, *S. aureus* TezR_D1^d, *S. aureus* TezR_R1^d or *S. aureus* TezR_D1/R1^d. Mice (n = 8) were
582 euthanized 12 h after inoculation and *ex vivo* CFU were determined in (B) abdominal fluid, (C)
583 liver, (D) spleen, and (E) kidneys. Values represent the mean \pm SD. Each symbol corresponds to
584 an individual mouse; horizontal bars denote the geometric mean. * $p < 0.05$, ** $p < 0.001$.
585

586 Formation of bacterial persisters can be modulated by TezRs

587 To gain insight into how TezRs regulated the formation of persisters, we used *E. coli* ATCC 25922.
588 Control *E. coli*, *E. coli* TezR_D1^d, *E. coli* TezR_R1^d, and *E. coli* TezR_D1/R1^d were normalized
589 with respect to CFU, diluted in fresh ampicillin-containing medium, and incubated for 6 h (Fig. 14).
590 The number of viable cells in the culture was determined by plating them on agar and overnight
591 incubation.



592

593 **Figure 14.** Impact of TezRs on persister formation.

594 Control *E. coli*, *E. coli* TezR_D1^d, *E. coli* TezR_R1^d, and *E. coli* TezR_D1/R1^d were exposed to
595 ampicillin for 6 h at 37 °C in LB broth and plated on LB agar without antibiotics to monitor CFU
596 counts and colony growth. Values are representative of three independent experiments. Bars
597 represent the mean \pm SD. * $p < 0.05$.

598

599 As expected, only 1/1304 of original control *E. coli* cells were ampicillin tolerant. Primary TezRs
600 regulated the rate at which cells entered dormancy and defined the persistence rate. The number
601 of persisters was 155 times higher in *E. coli* TezR_D1^d and 8.5 times higher in *E. coli* TezR_R1^d
602 (Fig. 14). Notably, the combined loss of both primary DNA- and RNA-based TezRs did not affect
603 persister formation and there was no difference in the number of persisters between “drunk” *E.*
604 *coli* TezR_D1/R1^d and the control.

605 **TezRs regulate spontaneous mutagenesis**

606 Next, we examined how the destruction of different TezRs affected the rate of spontaneous
607 mutagenesis. In these experiments, we measured spontaneous mutation frequency to rifampicin
608 in *E. coli* ATCC 25922 by counting viable RifR mutants after cultivation on rifampicin-
609 supplemented agar plates (Table 1). Spontaneous mutagenesis was inhibited in *E. coli*
610 TezR_D1^d, meaning that loss of TezR_D1 blocked the occurrence of replication errors, while loss
611 of TezR_R1 did not affect this process. Surprisingly, the combined loss of TezR_D1/R1 triggered
612 spontaneous mutagenesis and led to significantly more RifR mutants in “drunk” *E. coli*
613 TezR_D1/R1^d.

614 **Table 1.** Role of TezRs in spontaneous RifR mutagenesis.

| Probe | RifR mutants per 9 log ₁₀ <i>E. coli</i> cells (mean ± SD) ^a | P value |
|---------------------------------------|--|---------|
| Control <i>E.coli</i> | 27 ± 5.79 | |
| <i>E.coli</i> TezR_D1 ^d | 0 ± 0 | 0.015 |
| <i>E.coli</i> TezR_R1 ^d | 34 ± 8.84 | 0.249 |
| <i>E.coli</i> TezR_D1/R1 ^d | 1050 ± 258.83 | 0.021 |

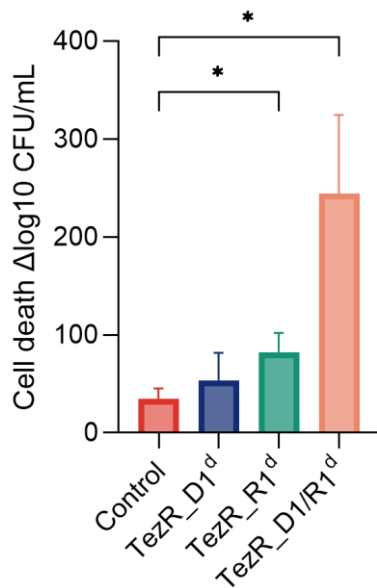
615 ^a Values represent the mean from at least three independent experiments.

616

617 **Loss of TezRs favors bacterial recombination**

618 To determine the role of TezRs in bacterial recombination, we incubated control *E. coli* LE392
619 with λ phage (bearing Ampr and Kanr genes) for a time sufficient to cause phage adsorption and
620 DNA injection. This was followed by treatment with nucleases to generate *E. coli* LE392
621 TezR_D1^d, *E. coli* LE392 TezR_R1^d, and *E. coli* LE392 TezR_D1/R1^d (61).

622 Control *E. coli* LE392 were incubated with λ phage, but were not treated with nucleases. Loss of
623 any primary TezRs increased recombination frequency, as indicated by the increased rate at
624 which phages lysogenized sensitive bacteria and, consequently, the higher number of antibiotic-
625 resistant mutants (Fig. 15). The increase was statistically significant ($p < 0.05$) only in bacteria
626 lacking TezR_R1 or those with combined loss of TezR_D1/R1. Taken together, these findings
627 show that primary TezRs regulate recombination frequency and their loss can affect prophage
628 formation.



629

630 **Figure 15.** Role of TezRs in bacteriophage integration frequency.

631 Data represent the mean of three independent experiments, error bars depict the standard
632 deviation. * $p < 0.05$.

633

634 **TezRs are required for chemosensing and utilization of xenobiotics**

635 To investigate the role of TezRs in xenobiotics sensing and utilization, control *B. pumilus* and *E.*
636 *coli* or their counterparts lacking primary TezRs were inoculated in M9 minimal medium
637 supplemented with the xenobiotic dexamethasone as the sole source of carbon and energy (62,
638 63). We compared the lag phase, which comprises the time required for sensing and starting the
639 utilization of these nutrients, between bacterial with unaltered and destroyed primary TezRs (64–
640 66).

641 Loss of TezR_D1 in *E. coli* and *B. pumilus* did not affect the lag phase when bacteria were grown
642 on media supplemented with dexamethasone. In marked contrast, the time lag of *E. coli* and *B.*
643 *pumilus* devoid of TezR_R1 (Fig. 16A, B) was delayed by 3 and 2 h compared with that of control
644 bacteria ($p < 0.05$), indicating a delay in the uptake and consumption of dexamethasone.

645 We hypothesized that the prolonged time required by bacteria lacking TezR_R1 to start using
646 dexamethasone resulted from disruption of their role in sensing and nutrient consumption, rather
647 than an alteration of transcriptional activity following their removal. To verify this hypothesis, we
648 conducted an experiment designed to prove that if bacteria used TezR_R1 to sense
649 dexamethasone, then *E. coli* pretreated with dexamethasone followed by TezR_R1 elimination
650 and cultivation in M9 supplemented with dexamethasone would have the same time lag as wild-
651 type *E. coli* in the same M9 medium. In other words, once bacteria sensed dexamethasone
652 through TezR_R1, they would continue responding to it even if TezR_R1 was subsequently
653 removed.

654 In agreement with this hypothesis, control *E. coli* exposed to dexamethasone for at least 20 min
655 with subsequent TezR_R1 loss and inoculation in dexamethasone-supplemented M9 exhibited
656 similar growth and time lag as control *E. coli* (Fig. 16C).

657 We also analyzed how loss of TezR_R1 altered the biochemical profile of *B. pumilus* grown on
658 minimal M9 medium supplemented with dexamethasone (Fig. 16D). Addition of dexamethasone
659 to control *B. pumilus* clearly induced a variety of enzymes known to participate in steroid
660 metabolism including β -glucuronidase (67). This increase was less apparent in *B. pumilus*
661 TezR_R1^d, whereby no β -glucuronidase was detected. Lack of changes to the biochemical
662 activity of bacteria devoid of TezRs following treatment with nutrients provides another line of
663 evidence supporting the essential role of TezRs in the sensing and response to chemical factors,
664 as well as recognition of xenobiotics.

665 **Utilization of lactose and functioning of the lac-operon are controlled by TezRs**

666 To evaluate the potential universal role of primary TezRs in detecting exogenous nutrients, we
667 examined their role in sensing lactose by cultivating the lac-positive strain *E. coli* ATCC 25922 in
668 M9 medium supplemented with lactose as the sole source of carbon and energy. Surprisingly,
669 unlike for dexamethasone, loss of TezR_R1 had no effect on lactose sensing. At the same time,
670 loss of TezR_D1 increased the time lag by 2 h compared with control *E. coli*, indicating how
671 utilization of lactose was regulated by these receptors (Fig. 16E). As with dexamethasone, when
672 control *E. coli* were pre-exposed to lactose for 20 min, followed by TezR_D1 removal and
673 subsequent cultivation on M9 medium supplemented with lactose, their behavior and time lag
674 was similar to that of control *E. coli* (Fig. 16F). This finding further confirmed the lactose-sensing
675 role of TezR_D1 and how functioning of the lac-operon relied on initial substrate recognition
676 through TezRs.

677 **TezRs are implicated in bacterial memory and forgetting**

678 We reasoned that, if TezRs participated in the sensing nutrients, they might also play a role in
679 bacterial memory formation and verified this possibility using an 'adaptive' memory experiment

680 (14, ⁶⁸). We found that control *E. coli* and *B. pumilus* “remembered” the first exposure to
681 dexamethasone, as indicated by shortening of the lag phase from 3 h upon first exposure to 2 h
682 upon second exposure for *E. coli* and from 5 to 2 h for *B. pumilus* (Fig. 16G, H).

683 We next assessed whether TezRs implicated in the memorization of a previous engagement to
684 nutrients required less time to trigger utilization of such a nutrient upon repeated sensing. To
685 achieve the stated goal, we exposed “dexamethasone-naïve” and “dexamethasone-sentient” *E.*
686 *coli* with unaltered TezRs to dexamethasone for different time periods. After that, TezR_R1 were
687 destroyed and cells were placed in fresh M9 medium containing dexamethasone. Only the
688 bacteria whose pre-exposure to dexamethasone prior to TezR_R1 destruction was enough to
689 trigger its utilization were able to grow. In agreement with our hypothesis, we found that TezR_R1
690 required 20 min to sense and trigger the utilization of dexamethasone upon first exposure to it
691 (Fig. 16I), but only 10 min upon second exposure ($p < 0.05$). The difference in time required for
692 TezR_R1 to mount a response at first (20 min) and repeated (10 min) contact with
693 dexamethasone points to the involvement of TezRs and the TRB-receptor system in long-term
694 cell memory formation, enabling a faster response to repeated stimuli (⁶⁹).

695 We next studied the role of TezRs in “forgetting”. We supposed that because TezRs participated
696 in bacterial memory, their continued loss might result in no memory of past experiences, which
697 would reflect in a longer time lag.

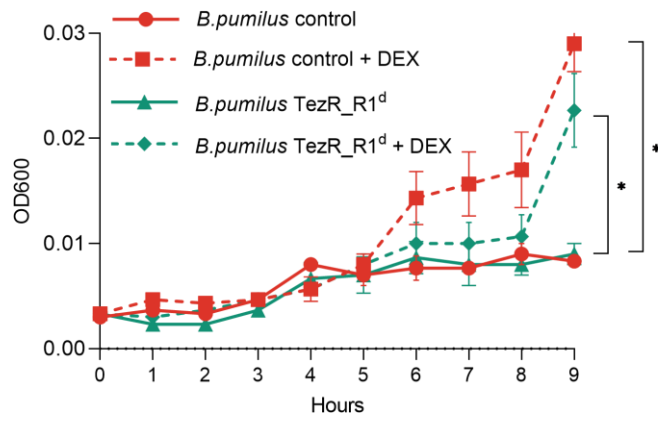
698 We found that control *B. pumilus* remembered the first exposure to dexamethasone, indicated by
699 reduction of the lag phase from 5 h upon first exposure to 2 h upon second exposure.
700 Dexamethasone-sentient *B. pumilus* with restored TezRs (following one- or two-time cycles of
701 TezRs removal and subsequent restoration) maintained a time lag below 2 h (Fig. 16J), meaning
702 that these one- or two-time cycles of TezRs loss did not affect bacterial memory. However, three
703 repeated rounds of TezRs removal and restoration led to “forgetting” of any previous exposure to
704 dexamethasone and the behavior of the corresponding *B. pumilus* became similar (5-h lag phase)
705 to that of control *B. pumilus* upon first exposure to dexamethasone. We named these cells, whose
706 memory had been erased by multiple cycles of TezRs loss “zero cells”.

707 Moreover, we found that after one or two-time removal of TezRs and subsequent restoration,
708 TezRs continued to react faster to the substrate than at the very first contact (Fig. 16K). However,
709 TezRs restored after three-time cycles destruction required the same contact time as naïve cells
710 to sense the substrate. We reasoned that TezRs restored after one- or two-time cycles of
711 destruction retained a type of “memory” (a reduced time required to sense and recognize
712 substrate). This phenomenon appeared to depend on the role of TezRs in a bacterial
713 intergenerational memory scheme capable of maintaining and losing past histories of interactions.

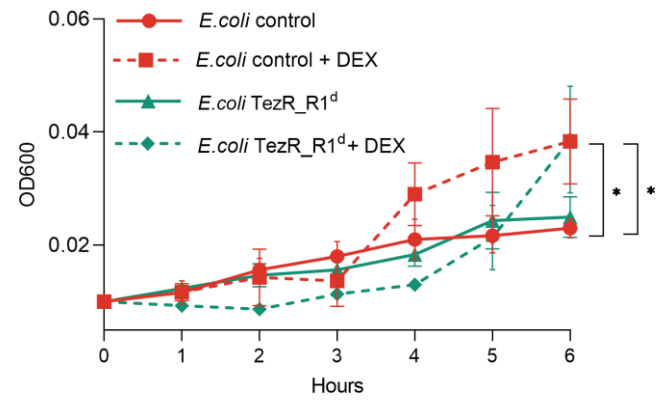
714

715

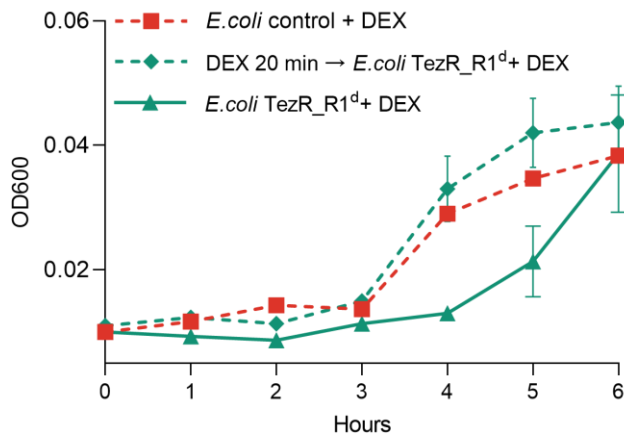
716



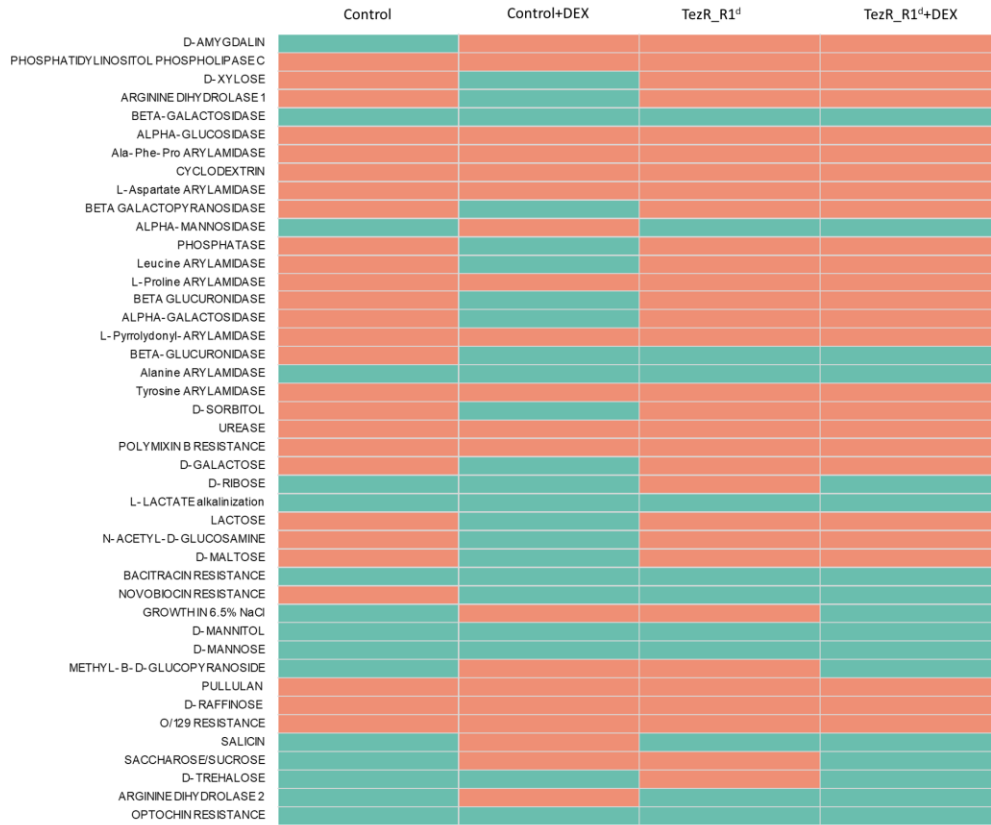
A



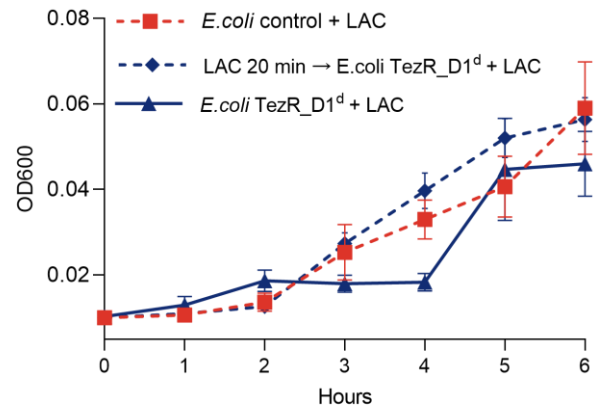
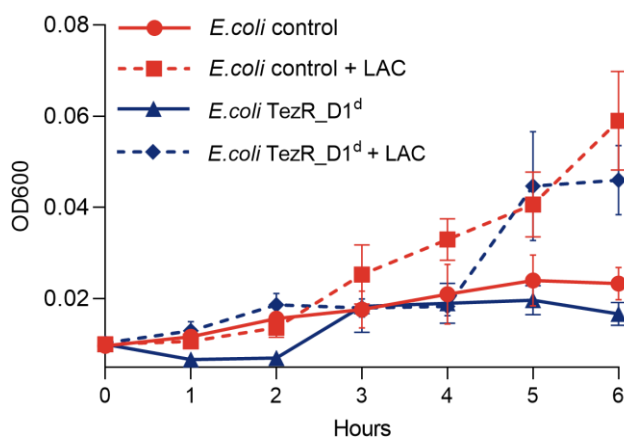
B



C

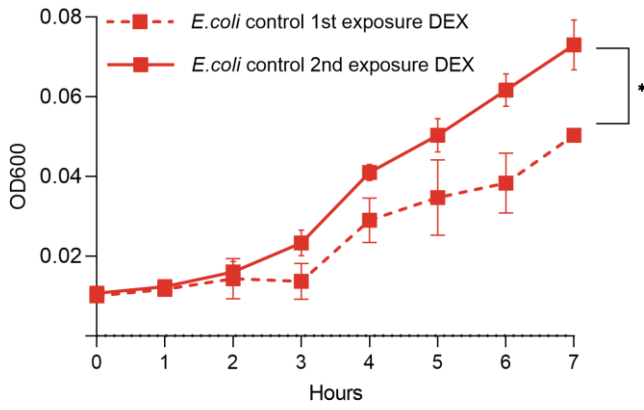


D

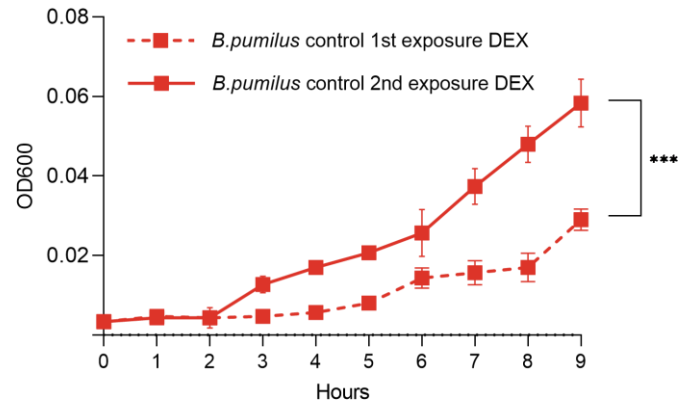


E

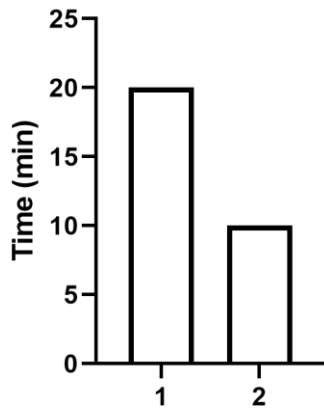
F



G



H



1: Minimal time required for TezR_R1 of dexamethasone-naive E. coli to start sensing dexamethasone

2: Minimal time required for TezR_R1 of dexamethasone-sensitized E. coli to start sensing dexamethasone

717

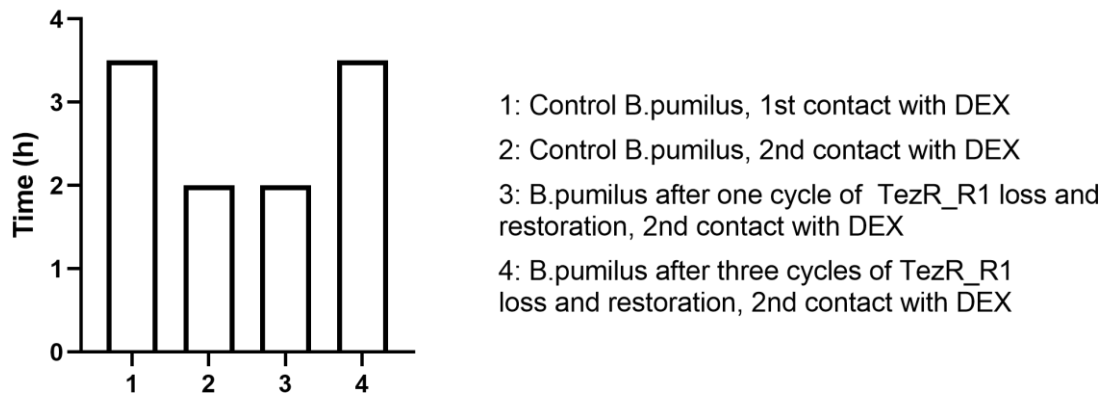
718 I

719

| | DEX 1 st exposure | D | R | M9 broth 1 st passage | D | R | M9 broth 2 nd passage | D | R | M9 broth 3 rd passage | M9 broth 4 th passage | DEX 2 nd exposure | 1 st exposure to Dex | Passage in LB broth | | | | 2 nd exposure to Dex | t _{lag} | | |
|-----------------------|------------------------------|--------|---|----------------------------------|--------|---|----------------------------------|--------|---|----------------------------------|----------------------------------|------------------------------|---------------------------------|---------------------|-----------------|-----------------|-----------------|---------------------------------|------------------|----|----|
| | | 30 min | | | 30 min | | | 30 min | | | | | | 1 st | 2 nd | 3 rd | 4 th | | 0h | 5h | |
| Control | + | - | - | + | - | - | + | - | - | + | + | + | Dark | Light | Light | Light | Light | Light | Dark | 0h | 5h |
| TezR_R1 ^{dz} | + | - | + | + | - | + | + | - | + | + | + | + | Dark | Light | Light | Light | Light | Light | Dark | 0h | 5h |

720

721 J



722

723 K

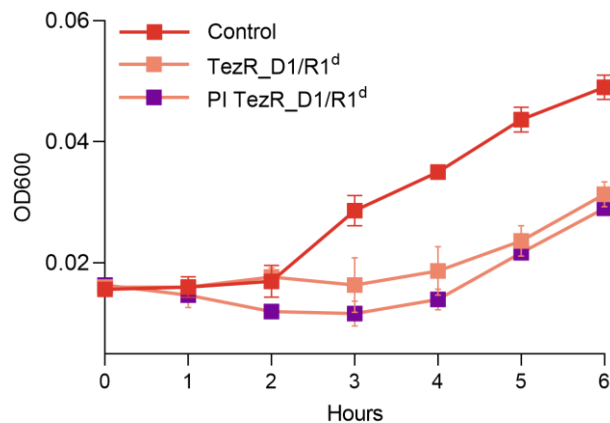
724

725 **Figure 15.** Role of TezRs in chemosensing and bacterial memory.

726 Growth of control *B. pumilus* or *E. coli* and their counterparts lacking primary TezRs on M9
727 medium with and without dexamethasone (DEX) or lactose (LAC) was monitored over time. (A)
728 Control *B. pumilus* and *B. pumilus* TezR_R1^d grown in M9 medium with or without
729 dexamethasone. (B) Control *E. coli* and *E. coli* TezR_R1^d grown in M9 medium with or without
730 dexamethasone. (C) Pretreatment of control *E. coli* with dexamethasone for 20 min followed by
731 TezR_R1 removal and subsequent growth on M9 medium supplemented with dexamethasone.
732 (D) Biochemical profile of control *B. pumilus* and *B. pumilus* TezR_R1^d grown on minimal M9
733 medium without (M9) or with dexamethasone (M9+DEX). Green denotes positive test reaction
734 results, red denotes negative results. Values show representative results of three independent
735 experiments. (E) Control *E. coli* and *E. coli* TezR_R1^d grown in M9 medium with or without lactose.
736 (F) Pretreatment of control *E. coli* with lactose for 20 min followed by TezR_R1 removal and
737 subsequent growth on M9 medium supplemented with dexamethasone. (G) Time required for
738 dexamethasone-naïve and dexamethasone-sentient control *E. coli* to commence growth on M9
739 medium supplemented with dexamethasone. (H) Time required for dexamethasone-naïve and
740 dexamethasone-sentient control *B. pumilus* to commence growth on M9 medium supplemented
741 with dexamethasone. (I) Minimal time required for TezR_R1 of *E. coli* to start sensing
742 dexamethasone. The X-axis represents the time lag of control *E. coli* upon initial and second
743 exposure to DEX. (J) Time to the start of DEX utilization (tlag) by dexamethasone-naïve and
744 dexamethasone-sentient *B. pumilus*. The experimental protocol is shown to the left. The tlag after
745 each passage in M9 medium with or without dexamethasone is shown to the right as a heat map,
746 whose color scale ranges from white (0 h) to red (5 h). (K) Minimal time required for TezR_R1 of
747 *B. pumilus* to start sensing dexamethasone.

748 **The effect of the binding of propidium iodine (PI) on the functionality of TezRs**

749 To further confirm the role of TezRs in cell signaling we inactivated them using PI, which is known
750 to bind both DNA and RNA without penetrating the live cells (70). Similar to the observation
751 where both TezR_D1/R1^d were removed, PI-treated *B. pumilus* exhibited the identical pattern of
752 increase in lag phase and delay in the uptake of dexamethasone when incubated in minimal
753 media (Fig. 17). Thus, these results imply that not only TezRs destruction, but also abrogation of
754 their functions by PI binding, modulates the sensory and regulatory activities of the cell.



755

756 **Figure 17.** Inactivation of TezRs with PI.

757 Time required for dexamethasone-sentient *B. pumilus* control (control), or *B. pumilus* following
758 TezR_D1/R1 destruction (TezR_D1/R1^d) or with TezR inactivated with PI (PI TezR_D1/R1^d) to
759 commence growth on M9 medium supplemented with dexamethasone.

760

761 **Role of reverse transcriptase and integrase in functioning of the TRB-receptor system**

762 We hypothesized that formation and functioning of TezRs could be associated with reverse
763 transcription and that affecting the corresponding enzymes might prevent the restoration of TezRs
764 after their removal. Recent data suggest that non-nucleoside reverse transcriptase inhibitors
765 (RTIs), originally designed to block HIV reverse transcriptase, interact non-specifically with
766 different transcriptases (71, 72). Here, we used non-nucleoside RTIs against control *S. aureus*
767 and *S. aureus* lacking primary TezRs.

768 The RTIs etravirine and nevirapine did not exhibit any antibacterial activity against *S. aureus* and
769 presented a MIC > 500 µg/mL (Supplementary Table 5). Thus, in this experiment we used very
770 low doses of RTIs, more than 100 fold lower than their MICs.

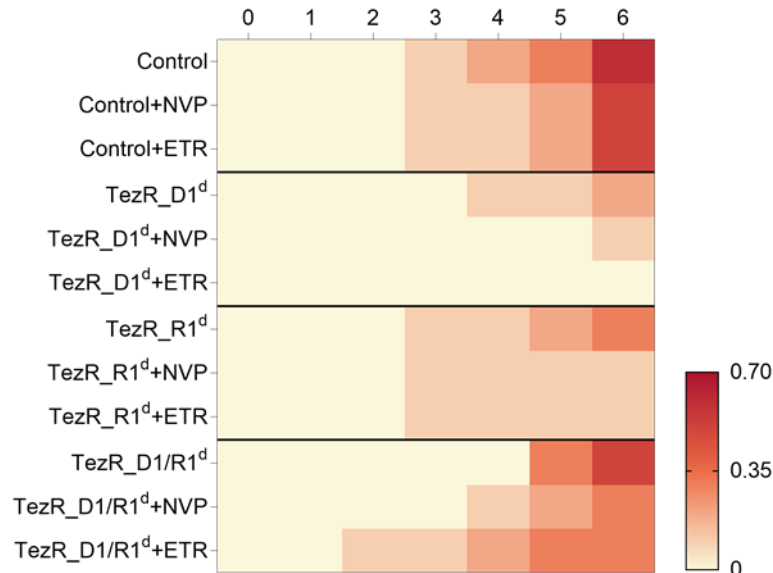
771 Addition of RTIs to the medium did not alter growth dynamics of control *S. aureus* (measured as
772 OD600), but affected growth of *S. aureus* lacking primary TezRs (Fig. 18A). Specifically, RTIs
773 inhibited growth of *S. aureus* TezR_D1^d ($p < 0.05$ for all), but not *S. aureus* TezR_R1^d. Even more

774 surprisingly, treatment of *S. aureus* TezR_D1/R1^d with RTIs accelerated bacterial growth. We
775 suggest that the inhibitory effect of RTIs on growth of bacteria lacking TezRs can be explained by
776 the requirement for these receptors when cells are grown in liquid media.

777 Next, we investigated the onset of a signal transduction cascade following the interaction between
778 TezRs and ligands. We hypothesized that the response to stimuli might also depend on
779 recombinases. To verify this possibility, we used raltegravir, an inhibitor of viral integrase known
780 to cross-react with bacterial recombinases due to structural and functional similarity with
781 HIV integrase (73, 74). Using a nontoxic concentration of raltegravir (Supplementary Table 5), we
782 successfully blocked the activation of bacterial enzymes of control *B. pumilus* in response to
783 dexamethasone (Fig. 18B). As a result, the biochemical profile of control *B. pumilus* grown on M9
784 medium supplemented with dexamethasone and raltegravir was almost identical to that of *B.*
785 *pumilus* grown on M9 without dexamethasone. This allowed us to assume that raltegravir blocked
786 signal transduction from TezRs following substrate recognition.

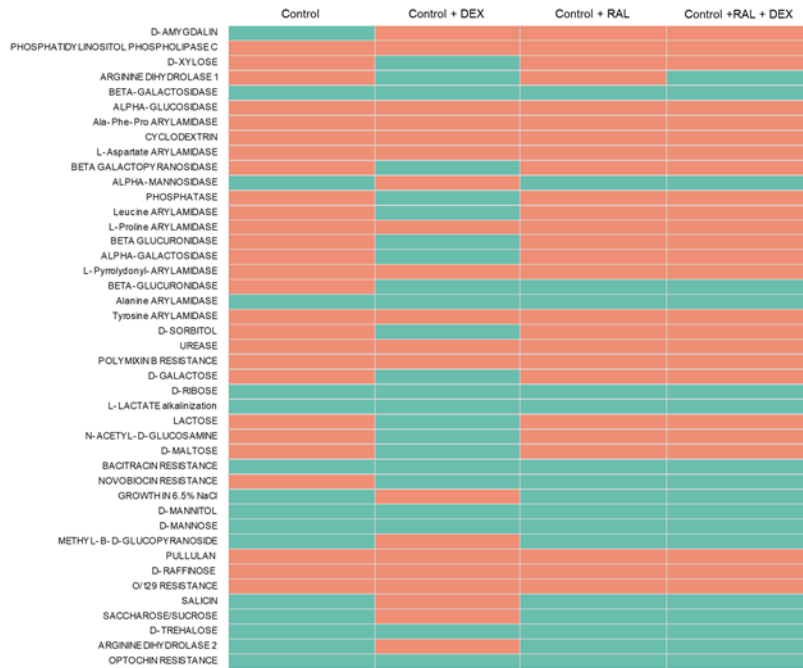
787 To confirm that the raltegravir-induced response of *B. pumilus* to dexamethasone was not the
788 result of any toxic effect, we measured OD600 of control *B. pumilus* when raltegravir was added
789 to the medium at different time points (Fig. 18C). Addition of raltegravir to dexamethasone-
790 sentient control *B. pumilus* grown on M9 with dexamethasone led to inhibition of bacterial growth
791 only when it was added together with the cells, but lost its inhibiting function if added 2 h after
792 growth had started (Fig. 18C). We believe that raltegravir inhibited signal transduction from TezRs
793 occurring during the first 2 h, but had no control over it once the signal had already been relayed.

794 Given that we previously showed how the loss of TezRs enhanced survival at higher
795 temperatures, we hypothesized that raltegravir might block signal transduction from TezRs and
796 lead to higher heat tolerance even in bacteria with intact TezRs. *S. aureus* treated or not with
797 raltegravir were gradually heated up to 65 °C and the presence of viable bacteria was analyzed.
798 *S. aureus* treated with raltegravir could survive at temperatures over 15 °C higher than those of
799 cells not treated with raltegravir (Fig. 18D). These data add another line of evidence supporting
800 the involvement of the TRB-receptor system in intracellular signal trafficking.



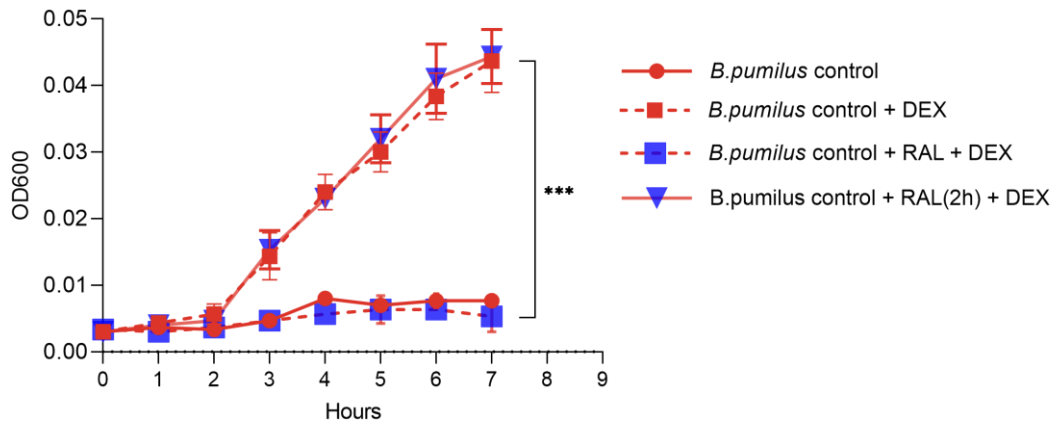
801

802 A



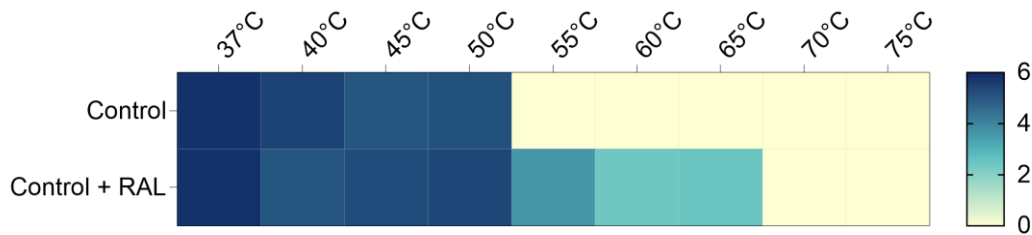
803

804 B



805
806

C



807

808 D

809

810 **Figure 18.** Role of reverse transcriptase and integrase in the TRB-receptor system.

811 (A) Effect of RTIs on bacterial growth and memory. Heat map representation of growth by control
812 *S. aureus*, *S. aureus* TezR_D1^d, *S. aureus* TezR_R1^d, and *S. aureus* TezR_D1/R1^d upon
813 treatment with RTIs. Nevirapine (NVP) and etravirine (ETR) were added to the broth and OD600
814 was monitored hourly for 6 h at 37 °C. OD600 is labeled by a color scale, from white (minimal) to
815 red (maximum). Values show representative results of three independent experiments. (B)
816 Biochemical profile of control *B. pumilus* grown on M9 minimal medium without (M9) or with
817 dexamethasone (M9+DEX), and with or without adding raltegravir (RAL). Green denotes positive
818 test reaction results, red denotes negative results. Values show representative results of three
819 independent experiments. (C) Raltegravir (RAL) added together with *B. pumilus* grown on M9
820 medium with dexamethasone (DEX) or 2 h after the plating of control *B. pumilus* on M9 with DEX
821 (blue triangles with red line). (D) Heat map showing the effect of raltegravir on signal transduction
822 from TezRs in relation to temperature tolerance in control and raltegravir-treated (control+RAL)
823 cells. CFU are labeled by a color scale, from white (minimum) to blue (maximum). Values show
824 representative results of three independent experiments.

825

826

827 **DISCUSSION**

828 Here, we describe for the first time the most external receptive system in bacteria, named “TRB-
829 receptor system”, which oversees almost all aspects of cell behavior and memory. Such a
830 universal receptive system, implicated in sensing a wide range of chemical, physical, and
831 biological factors, has not been described previously in eukaryotes or prokaryotes.

832 The system is composed of previously uncharacterized nucleic-acids based receptors capable
833 of sensory and regulatory function, as well as reverse transcriptases and integrases. Our study
834 shows a unique composition of these receptors, which we named TezRs. In contrast to known
835 receptors formed by proteins, TezRs are formed by DNA and RNA molecules (75). The selective
836 removal of different TezRs led to individual alterations in cell functioning and remarkably impacted
837 the transcription of various genes, which highlights the specific role of each of the discovered
838 TezRs.

839 We first showed that the TRB-receptor system functioned robustly across different bacterial types
840 and played a previously unexplored and critical role in the regulation of microbial growth in liquid
841 and solid media, as well as in collective behavior. These processes are known to be tightly
842 regulated by numerous genes and post-transcriptional events (76). Loss of different TezRs
843 resulted in changes to growth kinetics, biofilm formation, and cell size. The most significant
844 alterations were noted for biofilms formed by motile bacteria lacking TezR_D2. These biofilms
845 were characterized by formation of dendritic-like colony patterns, typical of cells with an increased
846 swarming motility (77). Given that swarming motility is a hallmark of bacterial multicellularity, it is
847 possible that TezRs participate in the regulation of this process (78).

848 Biofilm dispersal allows bacterial cells to leave a biofilm and migrate to a more favorable
849 environment for resettlement. Previous evidence suggests that biofilm dispersal is modulated by
850 the alteration of environmental conditions or gene activity (56, 80, 75). However, our data
851 validated that this process is also modulated by TezRs, without any other direct dependency on
852 exogenous or endogenous genetic stimulus.

853 Furthermore, we observed that TezRs controlled sporulation, which represents another important
854 bacterial indicator of the interaction with the external environment (81). The TRB-receptor system
855 exerted divergent effects on sporulation and loss of particular TezRs could either increase or
856 totally inhibit this process. Given that sporulation is a stressful event for the cell and its initiation
857 is tightly regulated in response to an unfavorable environment, increased sporulation following
858 loss of TezR_D1, TezR_R1, and particularly TezR_R2 raises the question of the role of these
859 TezRs in such context (82). The inhibition of sporulation following removal of TezR_D2 under
860 normal and stressful conditions adds another line of evidence suggesting that TezRs supervise
861 known regulatory pathways and known receptors responsible for sporulation.

862 We also found that primary TezRs regulated the rate at which cells entered dormancy and
863 determined the persistence rate, thus defining a bet-hedging strategy of cells. Even though the
864 molecular mechanisms underlying persister formation have been intensively studied and are
865 believed to be achieved through the modulation of multidrug efflux pumps, DNA repair, and ROS
866 production, as shown here the understanding of this important phenomenon is incomplete (83–
867 85).

868 To evaluate the role of the TRB-receptor system in bacterial adaptation to a variety of chemical
869 and physical factors, we began by looking at the regulation of bacterial survival at high
870 temperatures. In a set of experiments, we showed that all primary TezRs and TezR_R1 in
871 particular were key regulators of survival under thermal stress and their removal enabled cells to
872 tolerate up to 20°C higher temperatures than those managed by control bacteria. We reasoned
873 that, because loss of TezRs before the heating step but not after it increased survival, TezRs
874 might be involved in thermosensing and supervise the corresponding response. This idea was
875 supported by the notion that intracellular mRNA and RNA thermosensors could react to an altered
876 temperature, which thus modulated translation (86). We found that the TRB-receptor system
877 orchestrated the cell response to UV exposure. When bacteria are exposed to UV light, they
878 respond to DNA damage by a highly regulated series of events known as the SOS response,
879 which ultimately dictates whether the cell should survive or induce cell death (87, 88). Loss of
880 RNA-based TezRs increased survival after UV exposure, which can be explained by modulation
881 of SOS-induced cell death (89).

882 An interesting finding regarding the regulation of cell responses to variations in gas composition
883 was observed when the obligate aerobe *P. putida* could grow under anoxic conditions following
884 the removal of TezR_R1 or TezR_R2. Notably, this finding is echoed by recent theoretical studies
885 suggesting that growth of *P. putida* under anoxic conditions would require numerous additional
886 genes and a massive restructuring of its transcriptome to find alternative means of ATP synthesis
887 (46, 48). We reasoned that RNA-based TezRs could be implicated in sensing of the gas content
888 or stimulate genetic variability to enable the selection of clones capable of growing under anoxic
889 conditions.

890 Examining the bacterial response to other physical factors, we found that TezRs were involved in
891 sensing and regulation of the response to changes in the geomagnetic field (known as
892 magnetoreception) and light. Non-magnetotactic and non-photosynthetic *B. pumilus* with intact
893 TezRs sensed inhibition of the geomagnetic field and the presence of light in the environment, as
894 manifested by changes in biofilm morphology and expanded growth. We found that RNA-based
895 TezRs are implicated in sensing of the geomagnetic field and light and that, in the case of their
896 loss, bacteria could not start responding to alterations in these factors for a few hours, most likely
897 until these TezRs were restored. It is surprising, since until now, the identity of a magnetic sensor

898 in non-magnetotactic bacteria remained enigmatic; however, some studies show that different
899 bacteria even lacking magnetosomes are capable of sensing the geomagnetic field (25,26).

900 Interestingly, the ability of TezRs to interact with the magnetic field could be explained by the
901 nucleic-acid structure of these receptors, owing to the alleged paramagnetic properties of nucleic
902 acids and their ability to emit or transmit electromagnetic waves (90–94).

903 It has not escaped our attention that the observed altered responses to these physical factors by
904 bacteria lacking RNA-based TezRs happened only as long as DNA-based TezRs were present.
905 It is possible that different TezRs interact with each other to form functional complexes in which
906 they affect each other's functioning. This observation corroborates the fact that selective or
907 combined removal of various TezRs triggered different transcriptomic clustering. Notably, the
908 most significant impact on the transcriptome profiles, with the upregulation of the highest number
909 of genes was triggered by the individual loss of RNA-based TezRs.

910 Studying the role of the TRB-receptor system in response to different chemical and physical
911 factors, we were surprised by how cells lacking both RNA- and DNA-based TezRs continued
912 responding to some of these factors. Although TezR_D1/R1^d bacteria displayed an increased
913 survival at higher temperatures, their survival did not differ from that of control cells under altered
914 UV, light, and gas content conditions. Indeed, combined cleavage of different TezRs triggered
915 individual responses that were often more than just the sum of alterations triggered by the loss of
916 each individual TezR. Thus, we named cells lacking primary DNA- and RNA-based TezRs that
917 exhibited an unexpected response to stimuli “drunk cells.” The paradoxical behavior of “drunk
918 cells” could be explained by the existence of internal (i.e., cytoplasmic) TezRs (TezR_i), which
919 could be activated following the loss of primary TezRs. The existence of cytoplasmic receptors in
920 bacteria was only recently shown, but these receptors are protein-based and respond only to
921 chemosensing (95).

922 The present results also expanded our understanding of the TRB-receptor system in the control
923 of mutational events and recombination frequency. We found that TezRs regulated spontaneous
924 mutations and that it was possible to either inhibit this process through loss of TezR_D1 or
925 increase it via combined removal of TezR_D1/R1. We did not look deeper into this phenomenon;
926 however, we believe that alterations of these TezRs could possibly control the mismatch repair
927 system, which is known to be responsible for spontaneous mutagenesis (96). The control of
928 bacterial variability by the TRB-receptor system is also supported by increased recombination
929 frequency following TezRs destruction during infections of bacteria by phages (97).

930 Our findings support a role for TezRs in microbial virulence and pathogenicity. TezRs regulate
931 production of virulence factors, such as hemolysin and lecithinase, as well as *in vivo* bacterial
932 dissemination. These properties are known to play an important role in the spreading of infections,
933 but their underlying molecular mechanisms are only now beginning to be elucidated. In fact, given

934 that loss of TezRs inhibited bacterial dissemination, nucleases produced by macroorganisms
935 could actually constitute a protective mechanism (98, 99).

936 Finally, we studied the role of TezRs in bacterial chemotaxis, which is one of the primary means
937 of bacterial adaptation (37). We found that TezRs controlled chemotaxis and that removal of
938 certain TezRs could either promote or inhibit this process, or even cause a switch from positive
939 to negative chemotaxis. Because the loss of TezRs did not affect bacterial motility but modulated
940 chemotaxis, we conclude that TezRs control and oversee the function of transmembrane methyl-
941 accepting chemotaxis proteins, which are believed to be the primary regulators of chemotaxis
942 (100). In bacteria, chemotaxis can be viewed as an intrinsic element of chemoreception. Thus,
943 not surprisingly, we discovered that TezRs played a primary role in both processes. We found
944 that the existence of TezRs was a prerequisite for different bacteria to utilize well-recognized
945 factors such as lactose, as well as synthetic xenobiotics. The fact that lactose utilization, which is
946 one of the most well described examples of chemoreception, depends on TezRs can be explained
947 by the overseeing function of the TRB-receptor system over the lac-operon. We reasoned that
948 the controlling role of TezRs in sensing different substances including xenobiotics suggested how
949 different bacterial chemoreceptors were under the control of the TRB-receptor system.

950 The ability of cells to sense environmental factors and nutrients is also related to cell memory.
951 Participation of DNA- and RNA-based TezRs in cell memory formation to known nutrients and
952 xenobiotics was supported by the difference in time required to sense and trigger substrate
953 utilization by naïve and sentient bacteria. Given that genome rearrangement occurs during cell
954 memory formation, we suggested, and for the first time confirmed, that bacterial memory
955 formation could be blocked by recombinase inhibitors (101). Together, these results highlighted
956 how loss of TezRs could modulate genome rearrangement during bacterial memory formation
957 (101). Intriguingly, our results showed that TezRs of sentient bacteria exhibited faster substrate
958 recognition than naïve cells and that this difference could be passed on through multiple
959 generations. It is tempting to speculate that TezRs of sentient cells do not only maintain a memory
960 of previous interactions, but that they also exhibit faster substrate recognition, which implies a
961 selection of cells whose TezRs have higher affinity for previously encountered substrates. This
962 characteristic shares similarity with the adaptive strategy of immune cells, whose secondary and
963 more pronounced response is based on their affinity for antigens and the higher number of cells
964 possessing relevant receptors (102–104).

965 We hypothesized that cell memory formation included several processes. First, substrate is
966 sensed by TezRs. Second, this event triggers gene expression or rearrangement to utilize the
967 substrate. Third, TezRs with a memory of this substrate and ability to recognize it in follow-up
968 contacts are formed. The formation of TezRs with memory to previous events was proved by the
969 possibility to erase this memory via loss of TezRs in substrate-sentient cells. Indeed, three
970 repeated rounds of TezRs loss led to “forgetting” of the initial contact with the substrate. We

971 named such cells “zero cells”. “Zero cells” did not “remember” previous interactions with the
972 substrate and required the same time to start its utilization as substrate-naïve cells. We concluded
973 that removing TezRs and forming “zero cells” altered the activity of genes or triggered genetic
974 networks rearrangements. Therefore, we report for the first time that, by affecting TezRs, it is
975 possible to control memory formation and “forgetting”, both of which are critical aspects of memory
976 regulation. This finding opens a wide range of possibilities for directed cellular programming (105).

977 To address the question of how TezRs were formed, we hypothesized that this process involved
978 different types of DNA and RNA transcription events (106). Even though reverse transcriptases
979 have been found in a wide range of bacteria, their structure and function remain enigmatic (107).
980 Bacterial retroelements with reverse transcription activity (mainly represented by group II introns
981 associated with the CRISPR-Cas system), diversity-generating retroelements (producing
982 hypervariable proteins mediating adaptation to a changing environment), Abi-related reverse
983 transcriptases, and retron reverse transcriptases encoding extrachromosomal satellite multicopy
984 single-stranded RNA/DNA structures remain all poorly understood (108–111). In addition, there
985 are various reverse transcriptases of unknown function. In support of this idea, we observed
986 inhibition of bacterial growth when cells lacking primary DNA-based TezRs (and not control,
987 vehicle-treated cells) were treated with reverse transcriptase inhibitors. Accordingly, we
988 speculated that this occurred due to inhibition of TezRs restoration by reverse transcriptases.

989 We have not specifically investigated the mechanism of TezRs translocation to the cell surface,
990 but the observed upregulation of proteins associated with type VII secretion system (T7SS)
991 following the loss of DNA-based TezRs alone or in combination with RNA-based TezRs, raises
992 the question about T7SS involvement in translocation of DNA-based TezRs. Although, T7SS has
993 not yet been fully characterized, and the intricate molecular mechanisms underlying its function
994 remains elusive, the T7SS secretion machinery is attributed to bacterial pathogenicity and is also
995 known to be a part of curli biogenesis machinery that requires extracellular DNA (112, 113).

996 Trying to answer the question of how the signal from TezRs was processed further downstream
997 in the cells, we found that the integrase inhibitor raltegravir blocked the bacterial response to the
998 xenobiotic dexamethasone (74). As consumption of the latter was found to be controlled by
999 TezRs, this finding suggested that bacterial recombinases might be implicated in the processing
1000 of stimuli from TezRs. Taken together, these results allowed us to conclude that recombinases
1001 and reverse transcriptases were part of the TRB-receptor system.

1002 Taking into consideration the nucleic acids-based chemical nature of TezRs, it is worthwhile
1003 revisiting some of the existing paradigms of microbiology associated with nucleic acids. Thus,
1004 some biological effects so far associated with the action of nucleases against bacterial biofilms
1005 and inhibition of bacterial adhesion, might actually stem from previously overlooked changes to
1006 TezRs with subsequent loss of their receptive and regulatory function (44, 114, 115). Our data

1007 might also shed the light on the role of nucleic acids identified on cell surfaces, which have been
1008 described in some organisms but their contribution to cell functioning remained poorly defined
1009 (116–118).

1010 The model used in this study and based on the use of nucleases to remove TezRs relevant to
1011 natural conditions. Many bacteria secrete nucleases in the extracellular environment,
1012 suggesting that the destruction of TezRs may be a conserved and previously overlooked
1013 mechanism to gain a fitness advantage over competing strains (99, 119).

1014 Along with the nucleases we used PI which is known to bind both DNA and RNA without
1015 penetrating live cells (120). As expected, bacteria following PI treatment behaved similarly as the
1016 “drunk cells” after the destruction of primary DNA and RNA formed TezRs. Therefore, not only
1017 their destruction but also their inactivation due to PI binding could significantly affect the receptive
1018 and regulatory functions of TezRs.

1019 Future studies of the TRB-receptor system will require the development of new tools, coupled
1020 with an interdisciplinary approach that bridges microbiology and molecular biology. They should
1021 focus on the structural aspects of TezRs, as well as the molecular mechanisms of their formation
1022 and translocation to the cell surface. The functioning of bacterial TezRs across different
1023 organisms, as well as the mechanisms of their interaction with ligands and signal transduction
1024 should also receive attention.

1025 Considering the various cell features that are regulated by TezRs, we hypothesize that their
1026 specific functions stem from their physical characteristics, such as length and presence of specific
1027 loops or nucleic acids conformations (121, 122). A better understanding of these properties could
1028 lead to further and more accurate sub-classification of TezRs.

1029 In follow-up studies, it will be critical to pay attention to the association of primary and secondary
1030 TezRs with the cell surface, and the way signals from these TezRs are transmitted further
1031 downstream in the cells. Based on our data, we speculate that secondary TezRs may exist as
1032 free receptors not bound to cell structures. However, we could not determine how TezRs
1033 interacted with protein receptors performing the same function. One can assume that some
1034 TezRs might be an integral, sensing (i.e. ligand-binding) part of such a protein receptors.

1035 Moreover, given the recently discovered ability of DNA molecules to modify and misfold proteins,
1036 it is intriguing whether TezRs could possess a similar chaperoning function (27, 123–125).

1037 We are only starting to understand the sensory, receptive, and regulatory roles, as well as the
1038 structure of TezRs. Nevertheless, the need to deepen our knowledge in this field does not
1039 diminish the importance of the present observations. Finally, we believe that upcoming studies
1040 will expand our understanding of the whole set of sensing and regulatory processes involving
1041 TezRs.

1042 **Conclusion**

1043 In this study, we describe for the first time the most external bacterial receptive and regulatory
1044 system, which enables sensing and response to numerous chemical (including xenobiotics),
1045 physical, and biological stimuli. This system consists of DNA- or RNA-based receptors, which we
1046 termed TezRs and classified based on the type of nucleic acids and localization. Besides TezRs,
1047 the system includes also reverse transcriptases and integrases.

1048 Through removal of different TezRs, it is possible to modulate the cells' responses to external
1049 stimuli, as well as that of known receptor-mediated signaling pathways. Importantly, loss of TezRs
1050 can cause unexpected activity and rapid changes to cell properties; we termed these cells "drunk
1051 cells".

1052 We characterized also the role of TezRs in cell memory formation and maintenance. Importantly,
1053 by affecting the TRB-receptor system, it is possible to erase the memory of previous events,
1054 leading to "zero cells", whose existence opens new possibilities for regulating bacterial cells and
1055 populations.

1056 In summary, the discovered TRB-receptor system enables the regulation of diverse cellular
1057 processes, including those whose modulation was previously poorly explored. Crucially, it also
1058 enables bacteria to survive in the face of constant changes to surrounding environmental factors.

1059

1060 **MATERIALS AND METHODS**

1061 **Bacterial and phage strains and culture conditions**

1062 *Bacillus pumilus* VT1200, *Staphylococcus aureus* MSSA VT209, *Staphylococcus aureus* SA58-
1063 1, *Pseudomonas putida* VT085, and *Escherichia coli* LE392 infected with bacteriophage λ LZ1
1064 [gpD-GFP b::ampR, kanR] bearing ampicillin and kanamycin resistance were obtained from a
1065 private collection (provided by Dr. V. TRB). *Escherichia coli* ATCC 25922 was purchased from
1066 the American Type Culture Collection (Manassas, VA, USA). Bacterial strains were passaged
1067 weekly on Columbia agar (BD Biosciences, Franklin Lakes, NJ, USA) and stored at 4 °C. All
1068 subsequent liquid subcultures were derived from colonies isolated from these plates and were
1069 grown in Luria-Bertani (LB) broth (Oxoid, Hampshire, UK; Sigma-Aldrich, St Louis, MO, USA),
1070 Columbia broth (BD Biosciences) or nutrient broth (CM001; Oxoid), if not stated otherwise. Other
1071 liquid media included M9 Minimal Salts (Sigma-Aldrich). For experiments on solid media, bacteria
1072 were cultured on Columbia agar, nutrient agar (CM003; Oxoid), TGV agar (TGV-Dx, Human
1073 Microbiology Institute, New York, NY, USA), LB agar (Sigma-Aldrich), Aureus ChromoSelect Agar
1074 Base (Sigma-Aldrich), tryptic soy agar (Sigma-Aldrich), and egg-yolk agar (Hardy Diagnostics,
1075 Santa Maria, CA, USA). Sheep red blood cells were purchased from Innovative Research (Peary

1076 Court, MI, USA). All cultures were incubated aerobically at 37 °C in a
1077 Heracell 150i incubator (Thermo Scientific, Waltham, MA, USA) if not stated otherwise. For
1078 anaerobic growth experiments, *P. putida* VT085 was plated on agar and cultivated in AnaeroGen
1079 2.5-L Sachets (Oxoid) placed inside a CO₂ incubator (Sanyo, Kitanagoya, Aichi, Japan) at 37 °C
1080 for 24 h.

1081 Reagents

1082 Bovine pancreatic DNase I with a specific activity of 2,200 Kunitz units/mg and RNase A (both
1083 Sigma-Aldrich) were used at concentrations of 1 to 100 µg/mL. Ampicillin, kanamycin, rifampicin,
1084 vancomycin, nevirapine, etravirine, raltegravir, lactose, povidone iodine and dexamethasone
1085 were obtained from Sigma-Aldrich.

1086 Classification and nomenclature of TezRs

1087 We classified TezRs based on the structural features of their DNA- or RNA-containing domains,
1088 as well as association with the bacterial cell surface determined by the possibility of being washed
1089 into culture medium or matrix (Table 2).

1090 **Table 2.** Classification of TezRs in bacteria.

| Name of the receptor | Description of the receptor |
|----------------------|---|
| Primary TezRs | |
| TezR_D1 | DNA-based receptors located outside the membrane; they participate in cell regulation and are stably associated with the cell surface. |
| TezR_R1 | RNA-based receptors located outside the membrane; they participate in cell regulation and are stably associated with the cell surface. |
| Secondary TezRs | |
| TezR_D2 | DNA-based receptors located outside the membrane; they participate in cell regulation and can be easily washed out along with culture medium or matrix. |
| TezR_R2 | RNA-based receptors located outside the membrane; they participate in cell regulation and can be easily washed out along with culture medium or matrix. |

1091

1092 To describe bacteria with certain destroyed TezR, we marked them with the superscript letter “d”
1093 – meaning destroyed.

1094 An example of *E.coli* with destroyed primary DNA formed TezR will be designated as “E. coli
1095 TezR_D1^d”, where TezR stands for TRB receptor and is followed by an underscore, then a capital
1096 letter representing the type of nucleic acid (D for DNA), followed by an Arabic numeral
1097 representing that it is a primary receptor, and “d” superscript meaning that this receptor was
1098 destroyed. The same principle of naming is applicable for bacteria with other destroyed TezRs.
1099 Cells with multiple cycles of TezRs destruction and restoration were named “zero cells” and are
1100 designated by a superscript letter “z” placed after the letter “d”.

1101 **Removal of TezRs**

1102 To remove primary TezRs, bacteria were harvested by centrifugation at 4000 rpm for 15 min
1103 (Microfuge 20R; Beckman Coulter, La Brea, CA, USA), the pellet was washed twice in phosphate-
1104 buffered saline (PBS, pH 7.2) (Sigma-Aldrich) or nutrient medium to an optical density at 600 nm
1105 (OD600) of 0.003 to 0.5. Bacteria were treated for 30 min at 37 °C with nucleases (DNase I or
1106 RNase A), if not stated otherwise, washed three times in PBS or broth with centrifugation at
1107 4000 × *g* for 15 min after each wash, and resuspended in PBS or broth. Bacteria, whose TezRs
1108 were deleted or made non-functional, were marked with the superscript letter “d”.

1109 To study secondary TezRs, 1.5% TGV agar was used. After autoclaving at 121 °C for 20 min, the
1110 agar was cooled down to 45 °C and DNase I or RNase A, or a mixture of the two, was added,
1111 mixed, and 20 mL of the solution was poured into 90-mm glass Petri dishes.

1112 For biofilm formation assays, bacteria were separated from the extracellular matrix by washing
1113 three times in PBS or broth with centrifugation at 4000 × *g* for 15 min after each wash. Then, 25
1114 µL of suspension containing 7.5 log₁₀ cells was inoculated into the center of the prepared solid
1115 medium surface supplemented or not with nucleases and incubated at 37 °C for different times.

1116 **Inactivation of TezRs**

1117 To inactivate primary TezRs, bacteria were harvested by centrifugation at 4000 × *g* for 15 min
1118 (Microfuge 20R; Beckman Coulter, La Brea, CA, USA). The pellet was washed twice in PBS, pH
1119 7.2 (Sigma-Aldrich). Bacteria were treated with PI for 30 min at 37 °C. If not stated otherwise, the
1120 PI-treated cells were washed three times in PBS with subsequent centrifugation at 4000 × *g* for
1121 15 min, and resuspended in PBS or nutrient medium.

1122 **Growth curve**

1123 For growth rate determination at the various time points, stationary phase bacteria were washed
1124 from the extracellular matrix, treated with nucleases (10 µg/mL), and 5.5 log₁₀ cells were
1125 inoculated into 4.0 mL Columbia broth. OD600 was measured on a NanoDrop
1126 OneC spectrophotometer (Thermo Scientific).

1127 **Bacterial viability test**

1128 To evaluate bacterial viability, bacterial suspensions were serially diluted and 100 μ L of the diluted
1129 suspension was spread onto agar plates. Plates were incubated at 37 °C overnight and colony
1130 forming units (CFU) were counted the next day.

1131 **Biofilm morphology**

1132 To culture bacterial biofilms, we prepared glass Petri dishes containing TGV agar supplemented
1133 or not with 100 μ g/mL DNase I or RNase A, or a mixture of the two. Then, 25 μ L of a suspension
1134 containing 5.5 log₁₀ cells was inoculated in the center of the agar and the dishes were incubated
1135 at 37 °C for different times. The biofilms were photographed with a digital camera (Canon 6;
1136 Canon, Tokyo, Japan) and analyzed with Fiji/ImageJ software (126).

1137 **Fluorescence microscopy**

1138 Differential interference contrast (DIC) and fluorescence microscopy were used to confirm the
1139 destruction of primary TezRs with nucleases. Bacteria treated or not with nucleases were sampled
1140 at OD₆₀₀ of 0.1, washed from the matrix, fixed in 4% paraformaldehyde/PBS (Sigma-Aldrich) for
1141 15 min at room temperature, and stored at 4 °C until use. Bacteria were centrifuged at 14,000 \times
1142 *g* and cell pellets were dispersed in 10 μ L PBS, incubated with SYTOX Green at a final
1143 concentration of 2 μ M, and mounted in Fluomount mounting medium. Cells were imaged using
1144 an EVOS FL Auto Imaging System (Thermo Scientific) equipped with a 60 \times or 100 \times objective and
1145 2 \times digital zoom.

1146 Membrane-impermeable SYTOX Green stained cell surface-bound DNA and RNA. A reduction
1147 of green fluorescence compared to the untreated control, enabled the visualization of alterations
1148 elicited by nuclease treatment. Dead cells with permeable membranes showed a higher level of
1149 green fluorescence and were discarded from the analysis. No post-acquisition processing was
1150 performed; only minor adjustments of brightness and contrast were applied equally to all images.
1151 ImageJ software was used to quantify the signal intensity per cell; at least five representative
1152 images (60 \times field) were analyzed for each case (127).

1153 **Light microscopy-based methods**

1154 Samples were imaged on an Axios plus microscope (Carl Zeiss, Jena, Germany) equipped with
1155 an ApoPlan \times 100/1.25 objective. Images were acquired using a Canon 6 digital camera. Cell size
1156 was determined by staining cell membranes with methylene blue or Gram staining (both Sigma-
1157 Aldrich) and quantification in Fiji/ImageJ software. Values were expressed in px² (126).

1158 **Assays of RNase internalization**

1159 The internalization of RNase A was visualized in *B. pumilus*. *B. pumilus* (5.5 log₁₀ cells/ml) in PBS
1160 were incubated with fluorescein isothiocyanate (FITC) labeled RNase A at 37 °C for 15 or 60

1161 minutes as previously described (128). Bacteria were washed three times with PBS to remove
1162 any unbound protein. After washing the bacteria is cultivated for 2h in LB broth, washed to remove
1163 residual media components, and placed on a microscope slide for visualization. Fluorescence
1164 was monitored using a fluorescence microscope (Axio Imager Z1, Carl Zeiss, Germany). To
1165 visualize the internalization of RNase A, the biofilms of *B. pumilus* incubated with 100 µg/mL
1166 fluorescein-labeled RNase A were obtained as described earlier. After 24 h of growth at 37 °C,
1167 bacteria were washed three times with PBS to remove unbound proteins, and placed on a
1168 microscope to monitor the fluorescence using a fluorescence microscope (Axio Imager Z1, Carl
1169 Zeiss, Germany).

1170 **Generation of RNA sequencing data**

1171 To isolate RNA, the cell suspension obtained 2.5h post-nuclease treatment were washed thrice in
1172 PBS, pH 7.2 (Sigma) and centrifuged each time at 4000 × *g* for 15 min (Microfuge 20R,
1173 Beckman Coulter) followed by resuspension in PBS.

1174 RNA was purified using RNeasy Mini Kit (Qiagen) according to the manufacturer's protocol. The
1175 quantity and quality of RNA was spectrophotometrically evaluated by measuring the UV
1176 absorbance at 230/260/280 nm with the NanoDrop OneC spectrophotometer
1177 (ThermoFisher Scientific).

1178 Transcriptome sequencing (RNA-Seq) libraries were prepared using an Illumina TruSeq Stranded
1179 Total RNA Library Prep kit. RNA was ribodepleted using the Epicenter Ribo-Zero magnetic gold
1180 kit (catalog no. RZE1224) according to the manufacturer's guidelines. The libraries were pooled
1181 equimolarly and sequenced in an Illumina NextSeq 500 (Illumina, San Diego CA) platform with
1182 paired 150-nucleotide reads (130MM reads max).

1183 **Analysis of RNA sequencing data**

1184 Sequencing reads were mapped corresponding to the reference genome of *S. aureus* NCTC
1185 8325 (NCBI Reference Sequence: NC_007795), and expression levels were estimated using
1186 Geneious 11.1.5. Transcripts with an adjusted P value of < 0.05 and log₂ fold change value of ±
1187 0.5 were considered for significant differential expression. PCA, volcano plots and Euclidean
1188 distances plots were generated using the ggplot2 package in R, and the Venn diagram was
1189 obtained using BioVenn (129).

1190 **Sporulation assay**

1191 Sporulation was analyzed under the microscope by counting cells and spores in 20 microscope
1192 fields and three replicates. For each image, we calculated the number of spores and the number
1193 of cells. Then, we plotted the ratio of spores to the combined number of cells and spores in each

1194 bin. Sporulation under stress conditions was carried out by heating the bacterial culture at 42 °C
1195 for 15 min.

1196 **Modulation of thermotolerance**

1197 Overnight *S. aureus* VT209 cultured in LB broth supplemented or not with raltegravir (5 µg/mL)
1198 was separated from the extracellular matrix by washing in PBS and then diluted with PBS to
1199 OD600 of 0.5. Bacteria were left untreated or treated with nucleases to remove primary TezRs
1200 and 5.5 log₁₀ CFU/mL were placed in 2-mL microcentrifuge tubes (Axygen Scientific Inc., Union
1201 City, CA, USA). Each tube was heated to 37, 40, 45, 50, 55, 60, 65, 70 or 75 °C in a dry bath
1202 (LSETM Digital Dry Bath; Corning, Corning, NY, USA) for 15 min. After heating, control *S. aureus*
1203 were immediately treated with nucleases to delete primary TezRs, washed three times to remove
1204 nucleases, serially diluted, plated on LB agar, and the number of CFU was determined within 24
1205 h.

1206 **Modulation of thermotolerance restoration after TezRs loss**

1207 To determine the time it took for thermotolerance to be restored in bacteria following TezRs
1208 removal, overnight *S. aureus* VT209 cultures were treated with 10 µg/mL DNase I or RNase A, or
1209 a mixture of the two. Bacteria lacking TezRs were inoculated in LB broth and sampled hourly for
1210 up to 8 h. The samples were heated at the maximum temperature tolerated by the bacteria and
1211 viability was assessed as described in the previous section. Untreated *S. aureus* were used as a
1212 control and were processed the same way by heating at the lowest non-tolerable temperature,
1213 serially diluted, plated on LB agar, and assessed for CFUs within 24 h. Complete restoration of
1214 normal temperature tolerance coincided with growth inhibition at higher temperatures. The
1215 experiment was not extended beyond this time point.

1216 **Bacteriophage infection assay**

1217 An overnight *E. coli* LE392 culture was diluted 1:1000 and grown in liquid LB broth supplemented
1218 with 0.2% maltose and 10 mM MgSO₄ at 30 °C for 18–24 h, until OD600 of 0.4. Cells were
1219 separated from the extracellular matrix by three washes in PBS and centrifugation at 4000 × *g* for
1220 15 min and 20 °C after each wash, followed by resuspension in ice-cold LB broth supplemented
1221 with 10 mM MgSO₄ to OD600 of 1.0. Approximately 10 µL of plaque-forming units of the purified
1222 λ phage was added to 200 µL *E. coli* LE392 with intact TezRs. The suspension was incubated for
1223 30 min on ice and another 90 min at room temperature to ensure that the phage genome entered
1224 the cells (Single-Cell Studies of Phage λ: Hidden Treasures Under Occam's Rug). The remaining
1225 phages were removed by three washes in PBS and centrifugation at 4000 × *g* for 15 min and 20
1226 °C after each wash.

1227 Bacteria were treated with nucleases to destroy primary TezRs, followed by three centrifugation
1228 steps at 4000 x g for 15 min and 20 °C. Control *E. coli* were not treated with nucleases. After that,
1229 100 µL of bacterial suspension was plated as a lawn on LB agar supplemented with 10 µg/mL
1230 kanamycin and 100 µg/mL ampicillin, incubated for 24 h at 30 °C, and the number of Amp/Kanr
1231 colonies was determined.

1232 **Persister assay**

1233 *E. coli* ATCC 25922 were treated with nucleases to remove primary TezRs, inoculated in LB broth
1234 supplemented with ampicillin (150 µg/mL), and incubated at 37 °C for 6 h. Samples taken before
1235 and after incubation with ampicillin were plated on LB agar without antibiotics to determine the
1236 CFU (⁸⁵). The frequency of persisters was calculated as the number of persisters in a sample
1237 relative to the number of cells before antibiotic treatment in each probe.

1238 **Analysis of virulence factors production**

1239 *S. aureus* SA58-1 were treated with nucleases to remove primary TezRs and resuspended in
1240 PBS to 6.0 log₁₀ CFU/mL.

1241 The hemolytic test was performed as previously described with minor modifications (130). Briefly,
1242 bacterial cells were plated in the center of Columbia agar plates supplemented with 5% sheep
1243 red blood cells and incubated at 37 °C for 24 h. A greenish zone around the colony denoted α-
1244 hemolysin activity; whereas β-hemolysin (positive) and γ-hemolysin (negative) activities were
1245 indicated by the presence or absence of a clear zone around the colonies. The size of the
1246 hemolysis zone (in mm) was measured.

1247 Lecithinase activity by bacteria with intact TezRs or lacking TezRs was determined by plating
1248 cells on egg-yolk agar and incubation at 37 °C for 48 h. The presence of the precipitation zone
1249 and its diameter were evaluated (131).

1250 **UV assay**

1251 *S. aureus* VT209 were treated with nucleases to remove primary TezRs. Control probes were left
1252 untreated. Bacteria at 8.5 log₁₀ CFU/mL in PBS were added to 9-cm Petri dishes, placed under
1253 a light holder equipped with a new 254-nm UV light tube (TUV 30W/G30T8; Philips, Amsterdam,
1254 The Netherlands), and irradiated for different times at a distance of 50 cm. After treatment,
1255 bacteria were serially diluted, plated on nutrition agar plates, incubated for 24 h, and CFU were
1256 determined.

1257 **Animal models**

1258 All animal procedures and protocols were approved by the institutional animal care and use
1259 (IACUC) committee at the Human Microbiology Institute (protocol: # T-19-204) and all efforts were

1260 made to minimize animal discomfort and suffering. Adult C57BL/6 mice weighing from 18 to 20 g
1261 (Jackson Laboratories, Bar Harbor, ME, USA) were fed ad libitum and housed in individual cages
1262 in a facility free of known murine pathogens. Animals were cared for in accordance with National
1263 Research Council recommendations, and experiments were carried out in accordance with the
1264 Guide for the Care and Use of Laboratory Animals (132).

1265 Animals were randomly designated to four groups of eight mice each, which were used to
1266 measure the load of *S. aureus* SA58-1. Mice were anesthetized with 2% isoflurane, and
1267 intraperitoneally injected with nuclease-treated *S. aureus* at 10.1 log₁₀ to 10.2 log₁₀ CFU/mouse.
1268 Control animals received untreated *S. aureus* SA58-1. After 12 h, mice were euthanized by CO₂
1269 and cervical dislocation, and the bacterial load in the peritoneum, liver, spleen, and kidneys was
1270 determined by serial dilution and CFU counts after 48 h of culture on plates with selective *S.*
1271 *aureus* agar. Cell morphology was determined under an Axios plus microscope, following staining
1272 with a Gram stain kit (Merck, Darmstadt, Germany).

1273 **Magnetic exposure conditions**

1274 The effect of the TRB-receptor system on regulation of *B. pumilus* VT1200 growth when exposed
1275 to regular magnetic and shielded geomagnetic fields was assessed. *B. pumilus* lacking primary
1276 and secondary TezRs were obtained as previously discussed. Final inoculi of 5.5 log₁₀ CFU/mL
1277 in 25 µL were dropped in the center of agar-filled Petri dishes. Magnetic exposure conditions were
1278 modulated by placing the Petri dish in a custom-made box made of five layers of 10-µm-thick µ
1279 metal (to shield geomagnetic field) at 37 °C for 24 h. Biofilm surface coverage was analyzed using
1280 Fiji/ImageJ software and expressed as px² (127, 133).

1281 In a second experimental, *B. pumilus* VT1200 with intact TezRs and missing TezR_R1 were
1282 exposed to regular magnetic conditions or a shielded geomagnetic field as described above, and
1283 colony morphology was analyzed after 8 and 24 h. Images of the plates were acquired using a
1284 Canon 6 digital camera.

1285 **Estimation of spontaneous mutation rates**

1286 To calculate the number of mutation events, we used *E. coli* ATCC 25922, treated with nucleases
1287 to remove primary TezRs or untreated controls, and standardized at 9.0 log₁₀ cells. The number
1288 of spontaneous mutations to Rif^R was used to estimate the mutation rate. This was determined
1289 by counting the number of colonies formed on Mueller-Hinton agar supplemented or not with
1290 rifampicin (100 µg/mL). After incubation at 37 °C for 48 h, CFU as well as rifampicin resistant
1291 mutants were counted and the mutation rate was calculated by the Jones median estimator
1292 method (134).

1293 **Light exposure experiments**

1294 *B. pumilus* VT1200 lacking primary and secondary TezRs were obtained as described previously.
1295 An aliquot containing 5.5 log₁₀ bacteria in 25 µL was placed in the center of Columbia agar plates,
1296 which were then incubated at 37 °C for 7 or 24 h while irradiated with halogen lamps of 150 W
1297 (840 lm) (Philips, Shanghai, China). Colonies were photographed with a Canon 6 digital camera.
1298 The distance between the light source and the sample was 20 cm. Control probes were processed
1299 the same way, but were grown in the dark.

1300 **Chemotaxis and dispersal measurements**

1301 The assay was performed as described previously with some modifications. Briefly, assay plates
1302 containing TGV agar were prepared by adding 250 µL fresh human plasma to a sector comprising
1303 1/6 of the plate. The plasma was filtered through a 0.22-µm pore-size filter (Millipore Corp.,
1304 Bedford, MA, USA) immediately prior to use. Written informed consent was obtained from all
1305 patients to use their blood samples for research purposes, and the study was approved by the
1306 institutional review board of the Human Microbiology Institute (# VB-021420).

1307 *B. pumilus* VT1200 devoid of primary and secondary TezRs were obtained as described
1308 previously. An aliquot containing 5.5 log₁₀ cells in 25 µL was placed in the center of the plates,
1309 which were then incubated at 37 °C for 24 h and photographed with a Canon 6 digital camera.
1310 Chemotaxis was evaluated by measuring the migration of the central colony towards the plate
1311 sector containing plasma. Colony dispersal was assessed based on the appearance of small
1312 colonies on the agar surface.

1313 **Effect of reverse transcriptase inhibitors and integrase on bacterial growth**

1314 Minimum inhibitory concentrations (MICs) of nevirapine and etravirine against *S. aureus* VT209
1315 were evaluated. *S. aureus* VT209 with intact or missing primary TezRs were obtained as
1316 described previously. Bacteria were incubated in LB broth supplemented or not with nevirapine
1317 (5 µg/mL) or etravirine (5 µg/mL). These values corresponded to > 1/100 their MICs. Growth was
1318 monitored by measuring OD₆₀₀ during the first 6 h of incubation at 37 °C and recorded at hourly
1319 intervals on a NanoDrop OneC spectrophotometer.

1320 **Biochemical analysis**

1321 Biochemical tests were carried out using the colorimetric reagent cards GN (gram-negative) and
1322 BCL (gram-positive spore-forming bacilli) of the VITEK® 2 Compact 30 system (BioMérieux,
1323 Marcy l'Étoile, France) according to the manufacturer's instructions. The generated data were
1324 analyzed using VITEK® 2 software version 7.01, according to the manufacturer's instructions.

1325 **Recognition of lactose and dexamethasone**

1326 The role of the TRB-receptor system in the recognition of lactose and dexamethasone was
1327 investigated with *E. coli* ATCC 25922 and *B. pumilus* VT1200. Bacterial suspensions of control
1328 bacteria and those lacking primary TezRs were adjusted to a common CFU value and incubated
1329 in fresh M9 medium supplemented or not with 146 mM lactose or 127 mM dexamethasone.

1330 The lag phase, representing the period between inoculation of bacteria and the start of biomass
1331 growth, was measured by monitoring OD600. The lag phase reflects the time required for the
1332 onset of nutrient utilization (64, 65).

1333 **Cell memory formation experiments**

1334 The onset of bacterial memory was defined as the time required for dexamethasone to start being
1335 consumed (time lag) in dexamethasone-naïve and dexamethasone-sentient *B. pumilus* VT1200
1336 and *E. coli* ATCC 25922. To study the first exposure to dexamethasone, *B. pumilus* or *E. coli* with
1337 intact TezRs were incubated in fresh M9 medium supplemented or not with 127 mM
1338 dexamethasone for 24 h. To study the second exposure to dexamethasone, bacteria were taken
1339 after 24 h of cultivation from the first exposure to dexamethasone and washed three times in PBS
1340 with centrifugation at 4000 x g for 15 min and 20°C after each wash. Bacteria were adjusted to a
1341 common OD600 and incubated again in fresh M9 medium supplemented with dexamethasone.
1342 During the first and second exposures to dexamethasone, samples were taken at hourly intervals
1343 for the first 6 h and OD600 was measured with a NanoDrop OneC spectrophotometer to
1344 determine the lag phase. The different time lag between the first and second exposures to
1345 dexamethasone represented the formation of memory (135).

1346 **Evaluation of the role of TezRs in memory formation**

1347 To study the role of TezR_R1 in remembering previous exposures to nutrients, we assessed the
1348 difference in the time required for TezR_R1 of dexamethasone-naïve and dexamethasone-
1349 sentient *E. coli* ATCC 25922 to sense and trigger dexamethasone utilization. The two *E. coli* cell
1350 types with intact TezRs were pretreated with 127 mM dexamethasone for 5, 10, 15 or 20 min.
1351 Next, bacteria were treated with RNase A to remove TezR_R1, and inoculated in fresh M9
1352 medium supplemented with dexamethasone. The lag phase prior to dexamethasone consumption
1353 was determined by monitoring OD600 every hour.

1354 **Memory loss experiments**

1355 THE role of TezRs in bacterial memory loss was studied by comparing the lag phase of
1356 dexamethasone-naïve and dexamethasone-sentient *B. pumilus* VT1200 with intact TezRs (14).
1357 Bacteria were cultivated in M9 medium supplemented with 127 mM dexamethasone for 24 h,
1358 centrifuged at 4000 x g for 15 min, and washed in M9 medium without dexamethasone. The cells
1359 then underwent repeated rounds of TezR_R1 removal and restoration, followed by growth in M9
1360 broth without dexamethasone. After 24 h of cultivation at 37 °C, bacteria were isolated from the

1361 medium, TezR_R1 were removed again, and bacteria were re-inoculated in fresh M9 broth. In
1362 total, cultivation in M9 broth followed by TezR_R1 removal was repeated three times. Samples
1363 were taken prior to every TezR_R1 removal step, bacteria were washed, inoculated in M9 broth
1364 supplemented with dexamethasone, and the time lag to dexamethasone consumption was
1365 assessed by monitoring OD600.

1366 After the third set of cultivation in M9 broth, bacteria were centrifuged and inoculated in fresh M9
1367 broth. They were then cultivated for 24 h, centrifuged, washed, and inoculated in M9 broth
1368 supplemented with dexamethasone to mimic a second contact with dexamethasone. The time lag
1369 to dexamethasone consumption was assessed by monitoring OD600. Bacteria from the control
1370 group were processed the same way, but without undergoing TezR_R1 removal.

1371 **Raltegravir in cell memory formation experiments**

1372 The MIC of raltegravir against *S. aureus* VT209 was evaluated. To determine the effect of
1373 raltegravir on bacterial memory, *B. pumilus* VT1200 were grown on fresh M9 medium
1374 supplemented or not with 127 mM dexamethasone, with or without additionally supplementation
1375 with raltegravir (5 µg/mL, a 100-times lower concentration than the MIC). The biochemical profile
1376 of cells was analyzed with a VITEK® 2.

1377 To evaluate the maximal time required for raltegravir to affect dexamethasone utilization, *B.*
1378 *pumilus* VT1200 were grown in M9 broth supplemented with 127 mM dexamethasone, while
1379 raltegravir was added at 0 h, 15 min, 30 min, 1 h or 2 h. The samples were taken at hourly intervals
1380 for the first 6 h to measure OD600 and determine the lag phase.

1381 **Statistics**

1382 At least three biological replicates were performed for each experimental condition unless stated
1383 otherwise. Each data point was denoted by the mean value ± standard deviation (SD). A two-
1384 tailed *t*-test was performed for pairwise comparisons and $p \leq 0.05$ was considered significant.
1385 Bacterial quantification data were log₁₀-transformed prior to analysis. Statistical analyses for the
1386 biofilm assays and hemolysin test were performed using Student's *t*-test. Data from animal and
1387 sporulation studies were calculated using a two-tailed Mann-Whitney U test. GraphPad Prism
1388 version 9 (GraphPad Software, San Diego, CA, USA) or Excel 10 (Microsoft, Redmond, WA,
1389 USA) were applied for statistical analysis and illustration.

1390

1391 Supplementary Table 1. Effect of primary TezR_D1/R1 removal on bacterial size.

1392 Supplementary Table 2. Effect of primary TezRs removal on the size of *B. pumilus* VT1200
1393 biofilm.

1394 Supplementary Table 3. Effect of TezR removal on sporulation under normal conditions.

1395 Supplementary Table 4. Effect of TezR removal on sporulation under stress conditions.

1396 Supplementary Table 5. MICs of tested reverse transcriptase inhibitors and integrase inhibitor
1397 against control *S. aureus*.

1398 Supplementary Figure S1. Absence of RNase A internalization in *B. pumilus*.

1399 Supplementary Figure S2. Effect of TezRs removal on light sensing.

1400 **Author Contributions**

1401 VT and GT designed experiments. VT and GT supervised data analysis, analyzed data
1402 and wrote the manuscript.

1403

1404 **Competing interests**

1405 The authors declare no competing interests.

1406

1407 **ACKNOWLEDGMENTS**

1408 We gratefully acknowledge Dr. You Zhou, Microscopy facility at the Center for Biotechnology
1409 in University of Nebraska-Lincoln for help in microscopy; Kristina Kardava, Marya
1410 Vecherkovskaya and Tatiana Lazareva for setting some experiments; Genome Technology
1411 Center (GTC) for expert library preparation and sequencing, and the Applied Bioinformatics
1412 Laboratories (ABL) for providing bioinformatics support and helping with the analysis and
1413 interpretation of the data. GTC and ABL are shared resources partially supported by the
1414 Cancer Center Support Grant P30CA016087 at the Laura and Isaac Perlmutter Cancer Center.
1415 This work has used computing resources at the NYU School of Medicine High Performance
1416 Computing (HPC) Facility.

1417

1418

1419

1420

1421

1422 **References**

- 1423 1. Wadhams, G. H. & Armitage, J. P. Making sense of it all: bacterial chemotaxis. *Nat. Rev.*
1424 *Mol. Cell Biol.* **5**, (2004).
- 1425 2. Ortega, Á., Zhulin, I. B. & Krell, T. Sensory Repertoire of Bacterial Chemoreceptors.
1426 *Microbiol. Mol. Biol. Rev.* **81**, (2017).
- 1427 3. Bi, S., Jin, F. & Sourjik, V. Inverted signaling by bacterial chemotaxis receptors. *Nat.*
1428 *Commun.* **9**, (2018).
- 1429 4. Rayo, J., Amara, N., Krief, P. & Meijler, M. M. Live Cell Labeling of Native Intracellular
1430 Bacterial Receptors Using Aniline-Catalyzed Oxime Ligation. *J. Am. Chem. Soc.* **133**,
1431 7469–7475 (2011).
- 1432 5. Falke, J. J. & Hazelbauer, G. L. Transmembrane signaling in bacterial chemoreceptors.
1433 *Trends Biochem. Sci.* **26**, (2001).
- 1434 6. Ng, W.-L. *et al.* Probing bacterial transmembrane histidine kinase receptor-ligand
1435 interactions with natural and synthetic molecules. *Proc. Natl. Acad. Sci.* **107**, (2010).
- 1436 7. Falke, J. J. Cooperativity between bacterial chemotaxis receptors. *Proc. Natl. Acad. Sci.*
1437 **99**, (2002).
- 1438 8. Hazelbauer, G. L., Falke, J. J. & Parkinson, J. S. Bacterial chemoreceptors: high-
1439 performance signaling in networked arrays. *Trends Biochem. Sci.* **33**, (2008).
- 1440 9. Yang, Y. & Sourjik, V. Opposite responses by different chemoreceptors set a tunable
1441 preference point in *Escherichia coli* pH taxis. *Mol. Microbiol.* **86**, (2012).
- 1442 10. Machuca, M. A. *et al.* *Helicobacter pylori* chemoreceptor TlpC mediates chemotaxis to
1443 lactate. *Sci. Rep.* **7**, (2017).
- 1444 11. Li, H. & Wang, H. Activation of xenobiotic receptors: driving into the nucleus. *Expert Opin.*
1445 *Drug Metab. Toxicol.* **6**, (2010).
- 1446 12. Sourjik, V. & Berg, H. C. Functional interactions between receptors in bacterial
1447 chemotaxis. *Nature* **428**, (2004).
- 1448 13. Jacquin, J. *et al.* Microbial Ecotoxicology of Marine Plastic Debris: A Review on
1449 Colonization and Biodegradation by the “Plastisphere”. *Front. Microbiol.* **10**, (2019).
- 1450 14. Wolf, D. M. *et al.* Memory in Microbes: Quantifying History-Dependent Behavior in a

- 1451 Bacterium. *PLoS One* **3**, (2008).
- 1452 15. Kordes, A. *et al.* Establishment of an induced memory response in *Pseudomonas*
1453 *aeruginosa* during infection of a eukaryotic host. *ISME J.* **13**, (2019).
- 1454 16. Gosztolai, A. & Barahona, M. Cellular memory enhances bacterial chemotactic navigation
1455 in rugged environments. *Commun. Phys.* **3**, (2020).
- 1456 17. Andersson, S. G. E. Stress management strategies in single bacterial cells. *Proc. Natl.*
1457 *Acad. Sci.* **113**, (2016).
- 1458 18. Lambert, G. & Kussell, E. Memory and Fitness Optimization of Bacteria under Fluctuating
1459 Environments. *PLoS Genet.* **10**, (2014).
- 1460 19. Stock, J. B. & Zhang, S. The biochemistry of memory. *Curr. Biol.* **23**, (2013).
- 1461 20. Vashistha, H., Kohram, M. & Salman, H. Non-genetic inheritance restraint of cell-to-cell
1462 variation. *Elife* **10**, (2021).
- 1463 21. Yang, C.-Y. *et al.* Encoding Membrane-Potential-Based Memory within a Microbial
1464 Community. *Cell Syst.* **10**, (2020).
- 1465 22. Matsunaga, T. *et al.* Complete Genome Sequence of the Facultative Anaerobic
1466 Magnetotactic Bacterium *Magnetospirillum* sp. strain AMB-1. *DNA Res.* **12**, (2005).
- 1467 23. McCausland, H. C. & Komeili, A. Magnetic genes: Studying the genetics of
1468 biomineralization in magnetotactic bacteria. *PLOS Genet.* **16**, (2020).
- 1469 24. Scheffel, A. *et al.* An acidic protein aligns magnetosomes along a filamentous structure in
1470 magnetotactic bacteria. *Nature* **440**, (2006).
- 1471 25. Nordmann, G. C., Hochstoeger, T. & Keays, D. A. Magnetoreception—A sense without a
1472 receptor. *PLOS Biol.* **15**, (2017).
- 1473 26. Monteil, C. L. & Lefevre, C. T. Magnetoreception in Microorganisms. *Trends Microbiol.*
1474 **28**, (2020).
- 1475 27. Blank, M. & Goodman, R. DNA is a fractal antenna in electromagnetic fields. *Int. J.*
1476 *Radiat. Biol.* **87**, (2011).
- 1477 28. Berashevich, J. & Chakraborty, T. How the Surrounding Water Changes the Electronic
1478 and Magnetic Properties of DNA. *J. Phys. Chem. B* **112**, (2008).
- 1479 29. Nikiforov, V. N., Koksharov, Y. A. & Irkhin, V. Y. Magnetic properties of “doped” DNA. *J.*
1480 *Magn. Magn. Mater.* **459**, (2018).

- 1481 30. Yoney, A. & Salman, H. Precision and Variability in Bacterial Temperature Sensing.
1482 *Biophys. J.* **108**, (2015).
- 1483 31. Chursov, A., Kopetzky, S. J., Bocharov, G., Frishman, D. & Shneider, A. RNAtips:
1484 analysis of temperature-induced changes of RNA secondary structure. *Nucleic Acids*
1485 *Res.* **41**, (2013).
- 1486 32. Sengupta, P. & Garrity, P. Sensing temperature. *Curr. Biol.* **23**, (2013).
- 1487 33. Barria, C., Malecki, M. & Arraiano, C. M. Bacterial adaptation to cold. *Microbiology* **159**,
1488 (2013).
- 1489 34. Abatedaga, I. *et al.* Integration of Temperature and Blue-Light Sensing in *Acinetobacter*
1490 *baumannii* Through the BlsA Sensor. *Photochem. Photobiol.* **93**, 805–814 (2017).
- 1491 35. Golic, A. E. *et al.* BlsA Is a Low to Moderate Temperature Blue Light Photoreceptor in the
1492 Human Pathogen *Acinetobacter baumannii*. *Front. Microbiol.* **10**, (2019).
- 1493 36. Briegel, A. *et al.* New Insights into Bacterial Chemoreceptor Array Structure and
1494 Assembly from Electron Cryotomography. *Biochemistry* **53**, (2014).
- 1495 37. Bi, S. & Sourjik, V. Stimulus sensing and signal processing in bacterial chemotaxis. *Curr.*
1496 *Opin. Microbiol.* **45**, (2018).
- 1497 38. Parkinson, J. S., Hazelbauer, G. L. & Falke, J. J. Signaling and sensory adaptation in
1498 *Escherichia coli* chemoreceptors: 2015 update. *Trends Microbiol.* **23**, (2015).
- 1499 39. Beyer, Szöllössi, Byles, Fischer & Armitage. Mechanism of Signalling and Adaptation
1500 through the *Rhodobacter sphaeroides* Cytoplasmic Chemoreceptor Cluster. *Int. J. Mol.*
1501 *Sci.* **20**, (2019).
- 1502 40. Irigoyen, J. P., Muñoz-Cánoves, P., Montero, L., Koziczak, M. & Nagamine, Y. The
1503 plasminogen activator system: biology and regulation. *Cell. Mol. Life Sci.* **56**, (1999).
- 1504 41. Bohn, C. *et al.* Experimental discovery of small RNAs in *Staphylococcus aureus* reveals a
1505 riboregulator of central metabolism. *Nucleic Acids Res.* **38**, 6620–6636 (2010).
- 1506 42. Kengmo Tchoupa, A. *et al.* The type VII secretion system protects *Staphylococcus*
1507 *aureus* against antimicrobial host fatty acids. *Sci. Rep.* **10**, 14838 (2020).
- 1508 43. Taylor, J. C. *et al.* A type VII secretion system of *Streptococcus gallolyticus* subsp.
1509 *gallolyticus* contributes to gut colonization and the development of colon tumors. *PLOS*
1510 *Pathog.* **17**, e1009182 (2021).
- 1511 44. Whitchurch CB, T.-N. T. R. P. M. J. Extracellular DNA required for bacterial biofilm

- 1512 formation. *Science (80-.)*. **295**, 1487 (2022).
- 1513 45. Ingham, C. J. & Jacob, E. Swarming and complex pattern formation in *Paenibacillus*
1514 vortex studied by imaging and tracking cells. *BMC Microbiol.* **8**, (2008).
- 1515 46. Kampers, L. F. C. *et al.* A metabolic and physiological design study of *Pseudomonas*
1516 *putida* KT2440 capable of anaerobic respiration. *BMC Microbiol.* **21**, (2021).
- 1517 47. Glasser, N. R., Kern, S. E. & Newman, D. K. Phenazine redox cycling enhances
1518 anaerobic survival in *Pseudomonas aeruginosa* by facilitating generation of ATP and a
1519 proton-motive force. *Mol. Microbiol.* **92**, (2014).
- 1520 48. Nikel, P. I. & de Lorenzo, V. Engineering an anaerobic metabolic regime in *Pseudomonas*
1521 *putida* KT2440 for the anoxic biodegradation of 1,3-dichloroprop-1-ene. *Metab. Eng.* **15**,
1522 (2013).
- 1523 49. Eschbach, M. *et al.* Long-Term Anaerobic Survival of the Opportunistic Pathogen
1524 *Pseudomonas aeruginosa* via Pyruvate Fermentation. *J. Bacteriol.* **186**, (2004).
- 1525 50. Fuchs, S., Pané-Farré, J., Kohler, C., Hecker, M. & Engelmann, S. Anaerobic Gene
1526 Expression in *Staphylococcus aureus*. *J. Bacteriol.* **189**, (2007).
- 1527 51. Kadowaki, T. *et al.* *Porphyromonas gingivalis* Proteinases as Virulence Determinants in
1528 Progression of Periodontal Diseases. *J. Biochem.* **128**, (2000).
- 1529 52. Saunders, S. H. *et al.* Extracellular DNA Promotes Efficient Extracellular Electron
1530 Transfer by Pyocyanin in *Pseudomonas aeruginosa* Biofilms. *Cell* **182**, (2020).
- 1531 53. Ciemniecki, J. A. & Newman, D. K. The Potential for Redox-Active Metabolites To
1532 Enhance or Unlock Anaerobic Survival Metabolisms in Aerobes. *J. Bacteriol.* **202**, (2020).
- 1533 54. Rashid, M. H. & Kornberg, A. Inorganic polyphosphate is needed for swimming,
1534 swarming, and twitching motilities of *Pseudomonas aeruginosa*. *Proc. Natl. Acad. Sci.* **97**,
1535 (2000).
- 1536 55. Fraser, G. M. & Hughes, C. Swarming motility. *Curr. Opin. Microbiol.* **2**, (1999).
- 1537 56. Hagai, E. *et al.* Surface-motility induction, attraction and hitchhiking between bacterial
1538 species promote dispersal on solid surfaces. *ISME J.* **8**, (2014).
- 1539 57. Abee, T., Kovács, Á. T., Kuipers, O. P. & van der Veen, S. Biofilm formation and
1540 dispersal in Gram-positive bacteria. *Curr. Opin. Biotechnol.* **22**, (2011).
- 1541 58. Bartolini, M. *et al.* Regulation of Biofilm Aging and Dispersal in *Bacillus subtilis* by the
1542 Alternative Sigma Factor SigB. *J. Bacteriol.* **201**, (2019).

- 1543 59. McDougald, D., Rice, S. A., Barraud, N., Steinberg, P. D. & Kjelleberg, S. Should we stay
1544 or should we go: mechanisms and ecological consequences for biofilm dispersal. *Nat.*
1545 *Rev. Microbiol.* **10**, (2012).
- 1546 60. Velasco, E. *et al.* A new role for Zinc limitation in bacterial pathogenicity: modulation of α -
1547 hemolysin from uropathogenic *Escherichia coli*. *Sci. Rep.* **8**, (2018).
- 1548 61. Golding, I. Single-Cell Studies of Phage λ : Hidden Treasures Under Occam's Rug. *Annu.*
1549 *Rev. Virol.* **3**, (2016).
- 1550 62. Huang, Y. J. and B. L. . C32 LUNG INJURY, ARDS, AND SEPSIS: The Effects Of
1551 inhaled Glucocorticoids On Growth Of *Pseudomonas Aeruginosa*. *Am. J. Respir. Crit.*
1552 *Care Med.* 195 (2017).
- 1553 63. DeNiro, M. & Epstein, S. Mechanism of carbon isotope fractionation associated with lipid
1554 synthesis. *Science (80-)*. **197**, (1977).
- 1555 64. Paliy, O. & Gunasekera, T. S. Growth of *E. coli* BL21 in minimal media with different
1556 gluconeogenic carbon sources and salt contents. *Appl. Microbiol. Biotechnol.* **73**, (2007).
- 1557 65. Fernández de las Heras, L., García Fernández, E., María Navarro Llorens, J., Perera, J.
1558 & Drzyzga, O. Morphological, Physiological, and Molecular Characterization of a Newly
1559 Isolated Steroid-Degrading Actinomycete, Identified as *Rhodococcus ruber* Strain Chol-4.
1560 *Curr. Microbiol.* **59**, (2009).
- 1561 66. Basan, M. *et al.* A universal trade-off between growth and lag in fluctuating environments.
1562 *Nature* **584**, (2020).
- 1563 67. Shibasaki, H., Tanabe, C., Furuta, T. & Kasuya, Y. Hydrolysis of conjugated steroids by
1564 the combined use of β -glucuronidase preparations from *Helix pomatia* and *Ampullaria*:
1565 determination of urinary cortisol and its metabolites. *Steroids* **66**, (2001).
- 1566 68. Zarkan, A. *et al.* Indole Pulse Signalling Regulates the Cytoplasmic pH of *E. coli* in a
1567 Memory-Like Manner. *Sci. Rep.* **9**, (2019).
- 1568 69. Lyon, P. The cognitive cell: bacterial behavior reconsidered. *Front. Microbiol.* **6**, (2015).
- 1569 70. García-López, V. *et al.* Molecular machines open cell membranes. *Nature* **548**, 567–572
1570 (2017).
- 1571 71. Szilvay, A. M., Stern, B., Blichenberg, A. & Helland, D. E. Structural and functional
1572 similarities between HIV-1 reverse transcriptase and the *Escherichia coli* RNA
1573 polymerase β' subunit. *FEBS Lett.* **484**, (2000).

- 1574 72. Sciamanna, I., De Luca, C. & Spadafora, C. The Reverse Transcriptase Encoded by
1575 LINE-1 Retrotransposons in the Genesis, Progression, and Therapy of Cancer. *Front.*
1576 *Chem.* **4**, (2016).
- 1577 73. Spanopoulou, E. *et al.* The Homeodomain Region of Rag-1 Reveals the Parallel
1578 Mechanisms of Bacterial and V(D)J Recombination. *Cell* **87**, (1996).
- 1579 74. Nishana, M., Nilavar, N. M., Kumari, R., Pandey, M. & Raghavan, S. C. HIV integrase
1580 inhibitor, Elvitegravir, impairs RAG functions and inhibits V(D)J recombination. *Cell Death*
1581 *Dis.* **8**, (2017).
- 1582 75. Hershko, A. & Ciechanover, A. THE UBIQUITIN SYSTEM. *Annu. Rev. Biochem.* **67**,
1583 (1998).
- 1584 76. MartÃ-nez, L. C. & Vadyvaloo, V. Mechanisms of post-transcriptional gene regulation in
1585 bacterial biofilms. *Front. Cell. Infect. Microbiol.* **4**, (2014).
- 1586 77. Kearns, D. B. A field guide to bacterial swarming motility. *Nat. Rev. Microbiol.* **8**, (2010).
- 1587 78. Claessen, D., Rozen, D. E., Kuipers, O. P., Sogaard-Andersen, L. & van Wezel, G. P.
1588 Bacterial solutions to multicellularity: a tale of biofilms, filaments and fruiting bodies. *Nat.*
1589 *Rev. Microbiol.* **12**, (2014).
- 1590 79. Kaplan, J. B. Biofilm Dispersal: Mechanisms, Clinical Implications, and Potential
1591 Therapeutic Uses. *J. Dent. Res.* **89**, (2010).
- 1592 80. GÃvener, Z. T. & Harwood, C. S. Subcellular location characteristics of the *Pseudomonas*
1593 *aeruginosa* GGDEF protein, WspR, indicate that it produces cyclic-di-GMP in response to
1594 growth on surfaces. *Mol. Microbiol.* 071119190133004-??? (2007) doi:10.1111/j.1365-
1595 2958.2007.06008.x.
- 1596 81. Tetz, G. & Tetz, V. Introducing the sporobiota and sporobiome. *Gut Pathog.* **9**, 38 (2017).
- 1597 82. Errington, J. Regulation of endospore formation in *Bacillus subtilis*. *Nat. Rev. Microbiol.* **1**,
1598 117–126 (2003).
- 1599 83. Dubnau, D. & Losick, R. Bistability in bacteria. *Mol. Microbiol.* **61**, 564–572 (2006).
- 1600 84. Wilmaerts, D., Windels, E. M., Verstraeten, N. & Michiels, J. General Mechanisms
1601 Leading to Persister Formation and Awakening. *Trends Genet.* **35**, 401–411 (2019).
- 1602 85. Svenningsen, M. S., Veress, A., Harms, A., Mitarai, N. & Semsey, S. Birth and
1603 Resuscitation of (p)ppGpp Induced Antibiotic Tolerant Persister Cells. *Sci. Rep.* **9**, 6056
1604 (2019).

- 1605 86. Loh, E., Righetti, F., Eichner, H., Twittenhoff, C. & Narberhaus, F. RNA Thermometers in
1606 Bacterial Pathogens. *Microbiol. Spectr.* **6**, (2018).
- 1607 87. Krishna, S., Maslov, S. & Sneppen, K. UV-Induced Mutagenesis in Escherichia coli SOS
1608 Response: A Quantitative Model. *PLoS Comput. Biol.* **3**, e41 (2007).
- 1609 88. Wadhawan, S. & Gautam, S. Rescue of Escherichia coli cells from UV-induced death and
1610 filamentation by caspase-3 inhibitor. *Int. Microbiol.* **22**, 369–376 (2019).
- 1611 89. Erental, A., Kalderon, Z., Saada, A., Smith, Y. & Engelberg-Kulka, H. Apoptosis-Like
1612 Death, an Extreme SOS Response in Escherichia coli. *MBio* **5**, (2014).
- 1613 90. Irkhin, V. Y. & Nikiforov, V. N. Quantum effects and magnetism in the spatially distributed
1614 DNA molecules. *J. Magn. Magn. Mater.* **459**, 345–349 (2018).
- 1615 91. Savelyev, I.V., Zyryanova, N.V., Polesskaya, O.O. and Myakishev-Rempel, M., 2019. On
1616 the existence of the DNA resonance code and its possible mechanistic connection to the
1617 neural code. *NeuroQuantology*, 17(2), P. 56. & Savelyev IV, Zyryanova NV, Polesskaya
1618 OO, M.-R. M. On The Existence of The DNA Resonance Code and Its Possible
1619 Mechanistic Connection to The Neural Code. *NeuroQuantology* **17**, 56 (2019).
- 1620 92. Yi, J. Emergent paramagnetism of DNA molecules. *Phys. Rev. B* **74**, 212406 (2006).
- 1621 93. Montagnier, L., Aïssa, J., Ferris, S., Montagnier, J.-L. & Lavallée, C. Electromagnetic
1622 signals are produced by aqueous nanostructures derived from bacterial DNA sequences.
1623 *Interdiscip. Sci. Comput. Life Sci.* **1**, (2009).
- 1624 94. Zhang, Q., Throolin, R., Pitt, S. W., Serganov, A. & Al-Hashimi, H. M. Probing Motions
1625 between Equivalent RNA Domains Using Magnetic Field Induced Residual Dipolar
1626 Couplings: Accounting for Correlations between Motions and Alignment. *J. Am. Chem.*
1627 *Soc.* **125**, 10530–10531 (2003).
- 1628 95. Briegel, A. *et al.* Structure of bacterial cytoplasmic chemoreceptor arrays and implications
1629 for chemotactic signaling. *Elife* **3**, (2014).
- 1630 96. Schaaper, R. M. & Dunn, R. L. Spectra of spontaneous mutations in Escherichia coli
1631 strains defective in mismatch correction: the nature of in vivo DNA replication errors.
1632 *Proc. Natl. Acad. Sci.* **84**, (1987).
- 1633 97. Canchaya, C., Fournous, G., Chibani-Chennoufi, S., Dillmann, M.-L. & Brüssow, H.
1634 Phage as agents of lateral gene transfer. *Curr. Opin. Microbiol.* **6**, 417–424 (2003).
- 1635 98. Yang, D. *et al.* Human Ribonuclease A Superfamily Members, Eosinophil-Derived
1636 Neurotoxin and Pancreatic Ribonuclease, Induce Dendritic Cell Maturation and

- 1637 Activation. *J. Immunol.* **173**, 6134–6142 (2004).
- 1638 99. Sumbly, P. *et al.* Extracellular deoxyribonuclease made by group A Streptococcus assists
1639 pathogenesis by enhancing evasion of the innate immune response. *Proc. Natl. Acad.*
1640 *Sci.* **102**, (2005).
- 1641 100. Lux, R., Jahreis, K., Bettenbrock, K., Parkinson, J. S. & Lengeler, J. W. Coupling the
1642 phosphotransferase system and the methyl-accepting chemotaxis protein-dependent
1643 chemotaxis signaling pathways of Escherichia coli. *Proc. Natl. Acad. Sci.* **92**, (1995).
- 1644 101. Sheth, R. U. & Wang, H. H. DNA-based memory devices for recording cellular events.
1645 *Nat. Rev. Genet.* **19**, (2018).
- 1646 102. Kurosaki, T., Kometani, K. & Ise, W. Memory B cells. *Nat. Rev. Immunol.* **15**, 149–159
1647 (2015).
- 1648 103. McHeyzer-Williams, M., Okitsu, S., Wang, N. & McHeyzer-Williams, L. Molecular
1649 programming of B cell memory. *Nat. Rev. Immunol.* **12**, 24–34 (2012).
- 1650 104. Raychaudhuri, S. The Problem of Antigen Affinity Discrimination in B-Cell Immunology.
1651 *ISRN Biomath.* **2013**, 1–18 (2013).
- 1652 105. Chowdhury, S. *et al.* Programmable bacteria induce durable tumor regression and
1653 systemic antitumor immunity. *Nat. Med.* **25**, 1057–1063 (2019).
- 1654 106. Berg, P., Kornberg, R. D., Fancher, H. & Dieckmann, M. Competition between RNA
1655 polymerase and DNA polymerase for the DNA template. *Biochem. Biophys. Res.*
1656 *Commun.* **18**, (1965).
- 1657 107. Lim, D. & Maas, W. K. Reverse transcriptase in bacteria. *Mol. Microbiol.* **3**, (1989).
- 1658 108. Toro, N., Martínez-Abarca, F. & González-Delgado, A. The Reverse Transcriptases
1659 Associated with CRISPR-Cas Systems. *Sci. Rep.* **7**, (2017).
- 1660 109. Toro, N. & Nisa-Martínez, R. Comprehensive Phylogenetic Analysis of Bacterial Reverse
1661 Transcriptases. *PLoS One* **9**, e114083 (2014).
- 1662 110. Lampson, B. C., Inouye, M. & Inouye, S. Retrons, msDNA, and the bacterial genome.
1663 *Cytogenet. Genome Res.* **110**, (2005).
- 1664 111. Simon, D. M. & Zimmerly, S. A diversity of uncharacterized reverse transcriptases in
1665 bacteria. *Nucleic Acids Res.* **36**, (2008).
- 1666 112. Costa, T. R. D. *et al.* Secretion systems in Gram-negative bacteria: structural and
1667 mechanistic insights. *Nat. Rev. Microbiol.* **13**, 343–359 (2015).

- 1668 113. Erskine, E., MacPhee, C. E. & Stanley-Wall, N. R. Functional Amyloid and Other Protein
1669 Fibers in the Biofilm Matrix. *J. Mol. Biol.* **430**, 3642–3656 (2018).
- 1670 114. Tetz, G. V., Artemenko, N. K. & Tetz, V. V. Effect of DNase and Antibiotics on Biofilm
1671 Characteristics. *Antimicrob. Agents Chemother.* **53**, (2009).
- 1672 115. Guerrier-Takada, C., Gardiner, K., Marsh, T., Pace, N. & Altman, S. The RNA moiety of
1673 ribonuclease P is the catalytic subunit of the enzyme. *Cell* **35**, (1983).
- 1674 116. Huang, N. *et al.* Natural display of nuclear-encoded RNA on the cell surface and its
1675 impact on cell interaction. *Genome Biol.* **21**, (2020).
- 1676 117. Doyle, R. J., Koch, A. L. & Carstens, P. H. Cell wall-DNA association in *Bacillus subtilis*.
1677 *J. Bacteriol.* **153**, (1983).
- 1678 118. HALL, M. R., MEINKE, W., GOLDSTEIN, D. A. & LERNER, R. A. Synthesis of
1679 Cytoplasmic Membrane-associated DNA in Lymphocyte Nucleus. *Nat. New Biol.* **234**,
1680 227–229 (1971).
- 1681 119. Terekhov, S. S. *et al.* A kinase bioscavenger provides antibiotic resistance by extremely
1682 tight substrate binding. *Sci. Adv.* **6**, (2020).
- 1683 120. Rosenberg, M., Azevedo, N. F. & Ivask, A. Propidium iodide staining underestimates
1684 viability of adherent bacterial cells. *Sci. Rep.* **9**, 6483 (2019).
- 1685 121. Bacolla, A., Wang, G. & Vasquez, K. M. New Perspectives on DNA and RNA Triplexes
1686 As Effectors of Biological Activity. *PLOS Genet.* **11**, e1005696 (2015).
- 1687 122. Herbert, A. *et al.* Special Issue: A, B and Z: The Structure, Function and Genetics of Z-
1688 DNA and Z-RNA. *Int. J. Mol. Sci.* **22**, 7686 (2021).
- 1689 123. Tetz, G. & Tetz, V. Bacterial Extracellular DNA Promotes β -Amyloid Aggregation.
1690 *Microorganisms* **9**, (2021).
- 1691 124. Tetz, G. *et al.* Bacterial DNA promotes Tau aggregation. *Sci. Rep.* **10**, (2020).
- 1692 125. Tetz, V. & Tetz, G. Bacterial DNA induces the formation of heat-resistant disease-
1693 associated proteins in human plasma. *Sci. Rep.* **9**, (2019).
- 1694 126. Schindelin, J. *et al.* Fiji: an open-source platform for biological-image analysis. *Nat.*
1695 *Methods* **9**, (2012).
- 1696 127. Rueden, C. T. *et al.* ImageJ2: ImageJ for the next generation of scientific image data.
1697 *BMC Bioinformatics* **18**, (2017).

- 1698 128. Wang, X. *et al.* Hyaluronic acid modification of RNase A and its intracellular delivery
1699 using lipid-like nanoparticles. *J. Control. Release* **263**, 39–45 (2017).
- 1700 129. Hulsen, T., de Vlieg, J. & Alkema, W. BioVenn – a web application for the comparison
1701 and visualization of biological lists using area-proportional Venn diagrams. *BMC*
1702 *Genomics* **9**, 488 (2008).
- 1703 130. Manukumar, H. M. & Umesha, S. MALDI-TOF-MS based identification and molecular
1704 characterization of food associated methicillin-resistant *Staphylococcus aureus*. *Sci. Rep.*
1705 **7**, (2017).
- 1706 131. Bennett, R. W. & Monday, S. R. *S.aureus* in International handbook of foodborne
1707 pathogens. in (ed. Miliotis MD, B. J.) 41–59 (2003).
- 1708 132. *Guide for the Care and Use of Laboratory Animals*. (National Academies Press, 1996).
1709 doi:10.17226/5140.
- 1710 133. Choudhry, P. High-Throughput Method for Automated Colony and Cell Counting by
1711 Digital Image Analysis Based on Edge Detection. *PLoS One* **11**, (2016).
- 1712 134. Jones ME, T. S. R. A. Luria-Delbrück fluctuation experiments: design and analysis.
1713 *Genetics* **136**, 1209–1216 (1994).
- 1714 135. Zhu L, Y. Z. Y. Q. T. Z. M. L. S. Z. L. X. Degradation of dexamethasone by acclimated
1715 strain of *Pseudomonas Alcaligenes*. *Int. J. Clin. Exp. Med.* **8**, 10971 (2015).
- 1716